Tirzepatide modulates the regulation of adipocyte nutrient metabolism through long-acting activation of the GIP receptor

Regmi, A.; Aihara, E.; Christe, M.E.; Varga, G.; Beyer, T.P.; Ruan, X.P.; ... ; Roell, W.

Article

Cell Metabolism

Tirzepatide modulates the regulation of adipocyte nutrient metabolism through long-acting activation of the GIP receptor

Graphical abstract

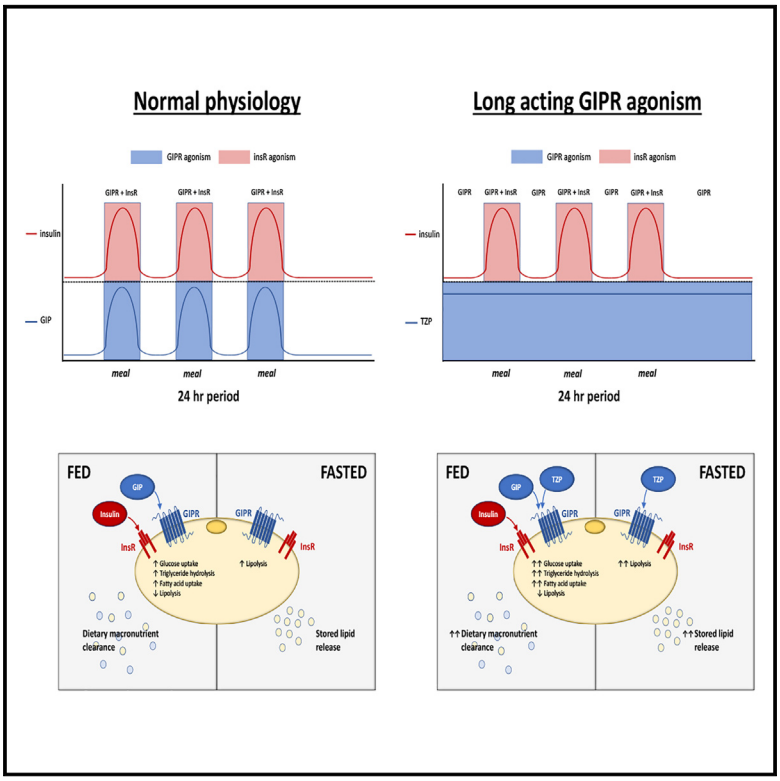

Highlights

- GIPR is expressed and functionally signals in both human and mouse adipocytes
- Tirzepatide signals to adipocytes via long-acting GIPR agonism
- Tirzepatide regulates adipocyte lipid and glucose storage as well as lipid efflux
- Tirzepatide regulation of adipocyte function likely contributes to overall efficacy

Authors

Ajit Regmi, Eitaro Aihara, Michael E. Christe, ..., Tamer Coskun, Melissa K. Thomas, William Roell

Correspondence

bill_roell@lilly.com

In brief

Tirzepatide, a novel long-acting GIPR/GLP-1R agonist, has recently demonstrated clinical efficacy in reducing HbA1c and body weight compared with placebo or selective GLP-1R agonists. Here, Regmi et al. identify mechanisms by which the long-acting GIPR agonism of tirzepatide may uniquely contribute to these clinical benefits by regulating adipocyte nutrient metabolism.

Regmi et al., 2024, Cell Metabolism *36*, 1534–1549
July 2, 2024
https://doi.org/10.1016/j.cmet.2024.05.010

CellPress

CellPress
OPEN ACCESS

Cell Metabolism

Article

Tirzepatide modulates the regulation of adipocyte nutrient metabolism through long-acting activation of the GIP receptor

Ajit Regmi,[1] Eitaro Aihara,[1] Michael E. Christe,[1] Gabor Varga,[1] Thomas P. Beyer,[1] Xiaoping Ruan,[1] Emily Beebe,[1] Libbey S. O'Farrell,[1] Melissa A. Bellinger,[1] Aaron K. Austin,[1] Yanzhu Lin,[1] Haitao Hu,[1] Debra L. Konkol,[1] Samantha Wojnicki,[1] Adrienne K. Holland,[1] Jessica L. Friedrich,[1] Robert A. Brown,[1] Amanda S. Estelle,[1] Hannah S. Badger,[1] Gabriel S. Gaidosh,[1] Sander Kooijman,[2] Patrick C.N. Rensen,[2] Tamer Coskun,[1] Melissa K. Thomas,[1] and William Roell[1,3,*]

[1]Eli Lilly and Company, Indianapolis, IN 46285, USA

[2]Department of Medicine, Division of Endocrinology, and Einthoven Laboratory for Experimental Vascular Medicine, Leiden University Medical Center, 2333 ZA Leiden, the Netherlands

[3]Lead contact

*Correspondence: bill_roell@lilly.com

https://doi.org/10.1016/j.cmet.2024.05.010

SUMMARY

Tirzepatide, a glucose-dependent insulinotropic polypeptide/glucagon-like peptide 1 receptor (GIPR/GLP-1R) agonist, has, in clinical trials, demonstrated greater reductions in glucose, body weight, and triglyceride levels compared with selective GLP-1R agonists in people with type 2 diabetes (T2D). However, cellular mechanisms by which GIPR agonism may contribute to these improved efficacy outcomes have not been fully defined. Using human adipocyte and mouse models, we investigated how long-acting GIPR agonists regulate fasted and fed adipocyte functions. In functional assays, GIPR agonism enhanced insulin signaling, augmented glucose uptake, and increased the conversion of glucose to glycerol in a cooperative manner with insulin; however, in the absence of insulin, GIPR agonists increased lipolysis. In diet-induced obese mice treated with a long-acting GIPR agonist, circulating triglyceride levels were reduced during oral lipid challenge, and lipoprotein-derived fatty acid uptake into adipose tissue was increased. Our findings support a model for long-acting GIPR agonists to modulate both fasted and fed adipose tissue function differentially by cooperating with insulin to augment glucose and lipid clearance in the fed state while enhancing lipid release when insulin levels are reduced in the fasted state.

INTRODUCTION

Chronic overnutrition and sedentary lifestyles have led to epidemic proportions of obesity, type 2 diabetes (T2D), and associated complications, including cardiovascular disease (International Diabetes Federation [IDF] Diabetes Atlas).[1] Lifestyle and therapeutic interventions often fail to substantially restore glucose control or maintain weight loss over time. New therapeutic approaches are needed to address these unmet medical needs. Tirzepatide, a novel long-acting glucose-dependent insulinotropic polypeptide receptor (GIPR)/glucagon-like peptide 1 receptor (GLP-1R) agonist, has recently demonstrated greater clinical efficacy in reducing HbA1c, body weight, and serum triglyceride levels as compared with placebo or selective GLP-1R agonists.[2–6] However, mechanisms by which combining GIPR with GLP-1R agonism improves clinical outcomes are incompletely understood.

Both GLP-1R and GIPR agonists enhance glucose-dependent insulin secretion from pancreatic beta cells, improving post-prandial glycemic control.[7,8] Additionally, engagement of GLP-1R and GIPRs expressed in the central nervous system has been proposed to reduce body weight through regulation of food intake.[9–12] Although dual receptor agonism may provide additive effects in conserved tissue/metabolic functions regulated similarly by both receptors, the substantial clinical improvements observed with adding GIPR to GLP-1R agonism suggest additional GIPR-mediated actions may provide unique contributions to improved nutrient disposition and metabolic control.

Adipose tissue is a potential direct mechanistic target of dual GIPR and GLP-1R agonists in contrast to GLP-1R monoagonists since GIPR (but not GLP-1R) is expressed in adipose tissue.[13] Preclinical and clinical studies suggest GIPR agonism may be an important regulator of adipose tissue function.[14] Adipose tissue is a key regulator of macronutrient partitioning, facilitating nutrient clearance and storage in the fed state and nutrient release in the fasted state, processes directly influenced by plasma insulin levels. As such, chronic GIPR agonism by tirzepatide may modulate both fasted and post-prandial adipocyte function differentially in the context of reduced and elevated

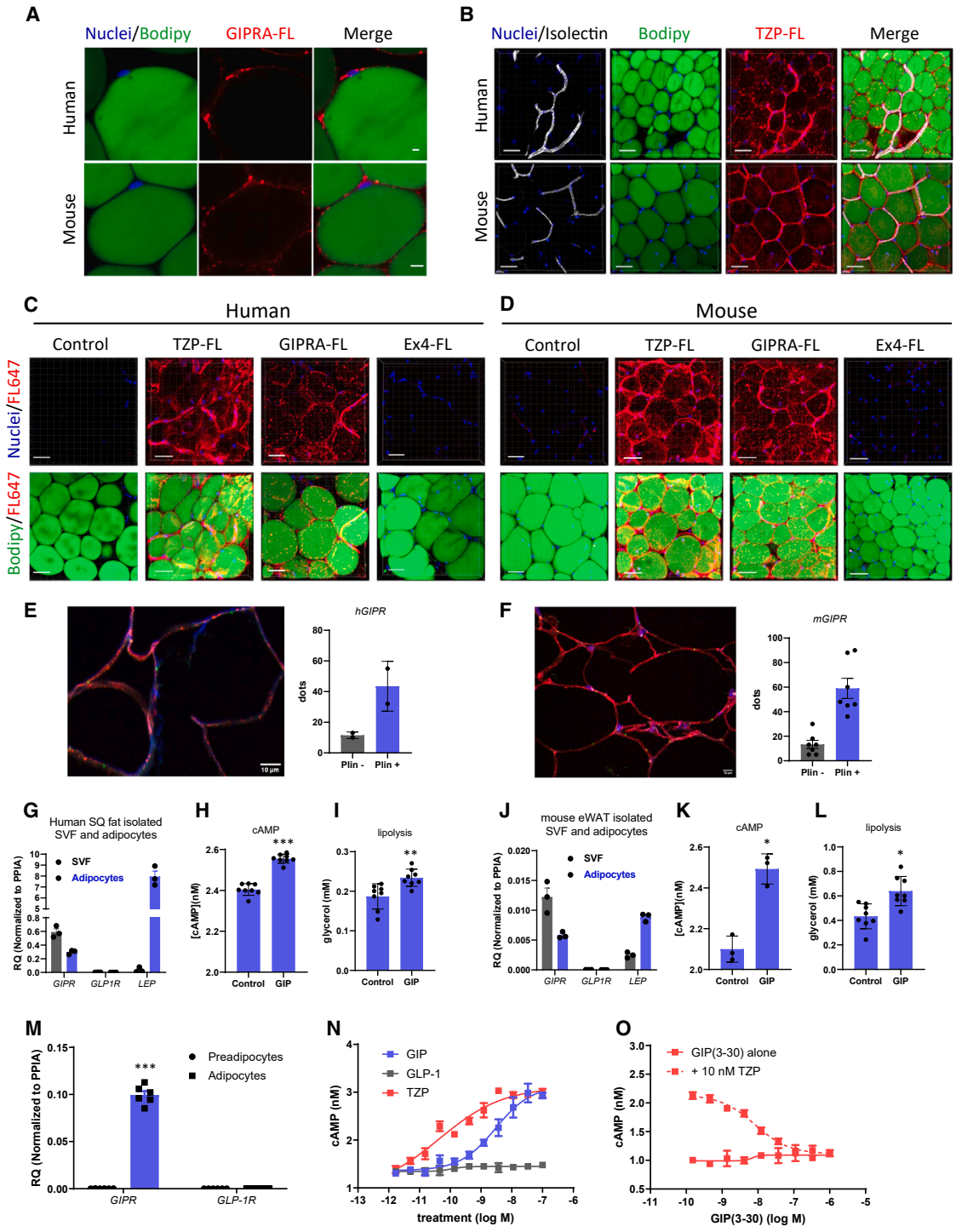

Figure 1. Tirzepatide signals via the GIPR expressed on human adipocytes

(A–D) Freshly isolated whole human or mouse adipose tissue incubated with fluorescently (red) labeled tirzepatide (TZP-FL), selective GIPR monoagonists (GIPRA-FL), or exendin-4 (Ex4-FL), followed by fixation and co-staining with Bodipy (green) and Hoechst 33342 (blue), with/without isolectin IB4 (white). Human and mouse adipocyte membrane localization of GIPRA-FL (A) and adipocyte and vascular localization of TZP-FL (B). Scale bars, 10 μm. Human (C) and mouse (D) adipose localization of TZP-FL and GIPRA-FL, but not Ex4-FL, on adipocytes in adipose tissue. Scale bars, 50 μm.

(E–L) RNAscope for GIPR expression (green) with perilipin (red) counter-staining to identify adipocytes on human (n = 2 biological samples) (E) and mouse (n = 7 biological samples) (F) adipose tissue with representative images and adipocyte and non-adipocyte fraction quantified expression. GIPR, GLP-1R, and leptin transcript expression assessed by Taqman in isolated adipocytes and SVF from human (n = 3 biological samples) (G) and mouse (n = 3 biological samples)

(legend continued on next page)

insulin signaling, respectively. However, a recent report employed genetically modified mouse models and single-cell RNA sequencing (scRNA-seq) analyses to suggest that GIPR may not be primarily expressed on adipocytes.[15,16] To address this question, we further characterized expression and functional regulation of GIPR on adipocytes in both human and mouse tissue. To evaluate tirzepatide regulation of adipocyte GIPR, we investigated actions of GIP and tirzepatide in human cellular and mouse models in the regulation of carbohydrate and lipid metabolism. The findings presented here elucidate potential mechanisms associated with the metabolic benefits of long-acting GIPR or dual GIPR/GLP-1R agonists. We further present a mechanistic model for the regulation of overall metabolic homeostasis via direct engagement of adipose tissue through the chronic GIP receptor agonism of tirzepatide.

RESULTS

Tirzepatide and selective GIPR monoagonist fluorescent tracers bind to adipocytes in human and mouse adipose

To identify whether tirzepatide engages adipocytes in adipose tissue, we engineered fluorescently labeled molecules to be used for imaging in whole adipose tissue: fluorescently labeled tirzepatide (TZP-FL), fluorescently labeled selective GIPR monoagonist (GIPRA-FL), and fluorescently labeled exendin-4 (Ex4-FL, a selective GLP-1R monoagonist) (Table S2). Briefly, whole adipose tissue was incubated with these fluorescently labeled molecules followed by fixation and incubation with Bodipy to label the adipocytes, Hoechst 33342 to label nuclei, and/or isolectin IB4 to label vasculature. Incubation of whole human and mouse adipose tissue demonstrated association of GIPRA-FL with adipocyte membranes (Figure 1A). Association of TZP-FL was observed with all adipocytes in human and mouse tissue and also along the vasculature (Figure 1B). When comparing TZP-FL and GIPRA-FL with Ex4-FL, both the tirzepatide and GIPR monoagonist tracers, but not the GLP-1R tracer, demonstrated association with all adipocytes (Figures 1C and 1D). These findings suggest that tirzepatide directly associates with adipocytes in adipose tissue via GIPR engagement.

GIPR is expressed and functionally active on adipocytes in human and mouse adipose

To further explore GIPR expression on adipocytes, we performed RNAscope using probes for GIPR mRNA in both human and mouse adipose. We identified the cytosolic compartment of adipocytes via fluorescent counter-staining of the intracellular lipid droplet protein perilipin. In both human (Figure 1E) and mouse (Figure 1F) adipose, GIPR transcript was observed in nearly all adipocytes, suggesting broad expression of GIPR in adipocytes. Additionally, GIPR transcript was observed in the non-adipocyte (perilipin-negative) cells as well, suggesting GIPR may be expressed in multiple cell types in adipose tissue. To evaluate these expression patterns more directly, we isolated both the mature adipocyte fraction and the stromal vascular fraction (SVF) from both human and mouse adipose and assessed GIPR and GLP-1R transcript expression, signal transduction, and regulation of function. GIPR, but not GLP-1R, transcript was expressed in both the SVF and adipocyte fractions of both human and mouse adipose (Figures 1G and 1J). To determine if GIP signaled on the isolated adipocytes, we treated human and mouse adipocytes with GIP and measured significant accumulation of cyclic AMP (cAMP), confirming direct functional engagement of GIPR on adipocytes (Figures 1H and 1K). Additionally, the expression and signaling of GIP on isolated adipocytes led to functional regulation as evidenced by stimulation of lipolysis (Figures 1I and 1L), an effect associated with GIP in other *in vitro* models.[17–19]

Differentiated human adipocytes express GIPR that is functionally activated by tirzepatide and GIP

To further investigate the regulation of adipocyte function by tirzepatide, we employed a human adipocyte model that was differentiated from human adipose-derived stromal cells. *In vitro* maturation increased mRNA expression levels of mature adipocyte markers (*CEBP*α, *PPAR*γ, and *AdipoQ*), multiple enzymes, and proteins essential for carbohydrate and lipid metabolism (e.g., *HSL*, *ATGL*, *FASN*, and *Glut4*) (Figure S1A) and produced morphologic changes consistent with adipocyte differentiation (Figure S1B). Differentiated cells expressed the insulin receptor (IR) and demonstrated appropriate time- and dose-responsive Akt phosphorylation in response to insulin (Figures S1C–S1E), providing an opportunity to study the effects of GIPR agonism in the presence and absence of insulin signaling to model fed and fasted conditions. Neither GIPR nor GLP-1R transcript expression was observed in the undifferentiated preadipocytes; however, GIPR, but not GLP-1R, expression was detected in differentiated adipocytes (Figure 1M). This pattern is consistent with previous findings[20] and suggests increasing levels of GIPR expression may be part of normal adipocyte maturation. Dose-response treatment with tirzepatide and GIP, but not GLP-1, stimulated cAMP accumulation (Figures 1N and S1F). Tirzepatide-dependent cAMP accumulation could be fully inhibited by co-treatment with the GIPR antagonist GIP(3–30)[21] (Figures 1O, S1G, and S1H).

Taken together, these findings suggest GIPR is expressed in both the adipocyte and non-adipocyte (SVF) fractions of human and mouse adipose tissue. This receptor expression on adipocytes is capable of signaling in response to GIP and regulating cellular functional responses. Further, these data demonstrate that tirzepatide engages adipocytes via GIPR but not GLP-1R and activates signaling through the GIPR. This suggests that

(J) adipose. cAMP accumulation and lipolysis in response to GIP treatment of isolated human (n = 8 technical replicates) (H and I) and mouse (n = 3 technical replicates cAMP, n = 8 technical replicates lipolysis; both from 3 pooled biological samples) (K and L) adipocytes.
(M–O) GIPR and GLP-1R transcript expression assessed by Taqman in undifferentiated and differentiated human adipocytes (n = 6 replicates) (M). cAMP accumulation (15 min treatment) in differentiated human adipocytes in response to GIP, tirzepatide, and GLP-1 (N). cAMP accumulation in differentiated adipocytes treated with TZP or TZP + GIPR antagonist GIP (3–30) (mean ± SEM, n = 3) (O).
Data are represented as mean ± SEM. $^{*}p < 0.05$, $^{**}p < 0.01$, $^{***}p < 0.001$ by Student's t test (H, I, and K–M). TZP, tirzepatide.
See also Figure S1.

tirzepatide may regulate adipocyte function via agonism at the GIPR.

Endogenous GIP is secreted by small intestinal K cells in response to nutrients and has a very short half-life in circulation of approximately 7 min in man,[22] effectively temporally restricting the duration of GIPR signaling to the timing around meals. By contrast, the long-acting GIPR agonist (LAGIPRA) tirzepatide has a mean half-life in humans of 116.7 h,[23] activating GIPR during meals, when both GIP and insulin signal to adipocytes, and during fasting conditions when endogenous GIP and insulin secretion levels are low. To investigate mechanisms by which tirzepatide regulates adipocyte function, GIPR agonism was studied in both the presence and absence of insulin to mimic fed or fasted conditions.

Concordant and discordant regulation of metabolic transcriptional pathways by GIPR agonism and insulin signaling in adipocytes

To identify mechanisms by which activation of GIPR and IR contribute to distinct and integrated regulation of carbohydrate and lipid metabolism in human adipocytes, we conducted mRNA expression profiling via exome array on adipocytes treated with GIP, insulin, GIP + insulin, or vehicle for 2, 8, and 24 h. Principal component analysis identified strong independent signatures from each of the treatments (Figure 2A). Differential mRNA expression patterns ($p < 0.05$; fold change ≥ 1.5 or ≤ -1.5) identified distinct and overlapping gene sets for further analysis (Figure 2B). Analyses of the 8 h time point illustrated robust differential regulation of mRNA expression by insulin and GIP and were used for subsequent pathway and regulator analyses from the array (Figures S2A–S2C).

We performed an upstream regulator assessment of transcription factors and nuclear hormone receptors predicted to be regulated by GIP, tirzepatide, or insulin in adipocytes. mRNA expression patterns associated with GIP treatment predicted modulation of key regulators of adipocyte function (e.g., CEBPα,β) (Figure S3) as well as regulatory networks typically associated with insulin signaling (e.g., FOXO1) (Figure S2D), demonstrating overlap of transcriptional regulation by insulin and GIPR agonism in adipocytes. Although several upstream regulators of adipocyte function were predicted to be more highly associated with GIP- (PPARδ, AP2) or insulin (PGC1β, SREBF2)-specific signaling, concordant regulation by GIP and insulin was observed for regulators of adipocyte differentiation (CEBPα/β), GPCR signaling (CREB), insulin signaling and glucose metabolism (FOXO1), lipid metabolism (PPARα, SREBF1), insulin sensitivity (PPARγ), and mitochondrial function (PGC1α) (Table 1). We performed RT-PCR to further evaluate mRNA expression levels of several of these master regulators of adipocyte function predicted from upstream analysis after treating adipocytes with vehicle, insulin, GIP, tirzepatide, GIP + insulin, or tirzepatide + insulin (Figures 2C–2L). GIPR activation by either GIP or tirzepatide significantly changed mRNA expression levels of *PPARα*, *PPARγ*, *PGC1α*, *CEBPα*, *CEBPβ*, *SREBP1*, *CREB*, and *FOXO1*, indicative of substantial regulation of macronutrient metabolism pathways. Although insulin demonstrated co-regulation of PPARα with GIP, it significantly counter-regulated GIP modulation of mRNA expression levels of *PPARγ*, *PGC1α*, *CEBPα*, *CEBPβ*, *SREBP1*, *CREB*, and *FOXO1*. These findings demonstrate overlapping modulation by GIP and insulin signaling pathways of key regulators of adipocyte function.

To further examine regulation of nutrient metabolic pathways by GIP independent of and combined with insulin, we conducted canonical pathway analysis of the exome array results. Carbohydrate metabolism pathways were highly regulated by GIPR agonism; for example, mRNA expression levels of multiple enzymes of the TCA cycle were upregulated by GIP and GIP + insulin but not by insulin alone (Figures 2M and S4), suggesting that GIP modifies adipocyte capacity to efficiently convert nutrients to energy stores. Triglyceride biosynthesis and degradation metabolic pathways were differentially regulated by GIPR as compared with IR agonism. mRNA expression levels of enzymes associated with triglyceride biosynthesis were primarily downregulated by GIP with some counter-regulation by insulin (Figures 2N and S5). Counter-regulation of triglyceride degradation pathways by insulin and GIP was also notable. Consistent with modulation of lipolysis, GIP increased and insulin decreased mRNA expression levels of multiple enzymatic regulators of the lipolysis pathway, including HSL, ATGL, and MGL (Figures 2O and S6). Of note, GIP potently upregulated mRNA expression of components of complexes 1–5 of the mitochondrial electron transport chain with evidence for counter-regulation by insulin signaling of expression levels of components of complexes 3 and 4 (Figures 2P and S7), suggestive of GIP-mediated modulation of adipocyte mitochondrial function and potential regulation of cellular energy balance.

These analyses of adipocyte master regulators and canonical pathways demonstrated that activation of GIPR signaling in the presence or absence of insulin signaling differentially regulates carbohydrate and lipid metabolism pathways. In this respect, GIP signaling may support a key metabolic function of adipose tissue to buffer macronutrient metabolism in both fed (glucose/lipid clearance) and fasted (hydrolysis and release of stored lipid) states with constitutive GIPR agonism. To better evaluate how such long-acting molecules such as tirzepatide differentially regulate adipocyte metabolism in the fed state (high plasma insulin) and fasted state (low plasma insulin) via GIPR agonism, we performed functional assays modeling carbohydrate and lipid metabolism in the human adipocyte model.

Tirzepatide and GIP increase insulin-dependent and -independent glucose uptake

Hierarchal clustering of gene sets associated with glucose metabolism curated using Ingenuity Pathway Analysis (IPA) and Kyoto Encyclopedia of Genes and Genomes (KEGG) pathways demonstrated similar differentially regulated mRNA expression patterns between GIP and insulin treatments (Figure S8A). To compare GIPR and IR activation regulation of glucose clearance into adipocytes, glucose uptake was evaluated by incorporation of ^{14}C-glucose into mature adipocytes. Acute treatment with insulin, GIP, and tirzepatide independently increased glucose transport into adipocytes in dose response, with insulin providing the greatest maximum glucose uptake (Figure 3A). When treated in combination with insulin, both tirzepatide and GIP significantly increased insulin-stimulated glucose uptake (Figure 3B), consistent with a direct insulin-sensitizing effect on human adipocytes.

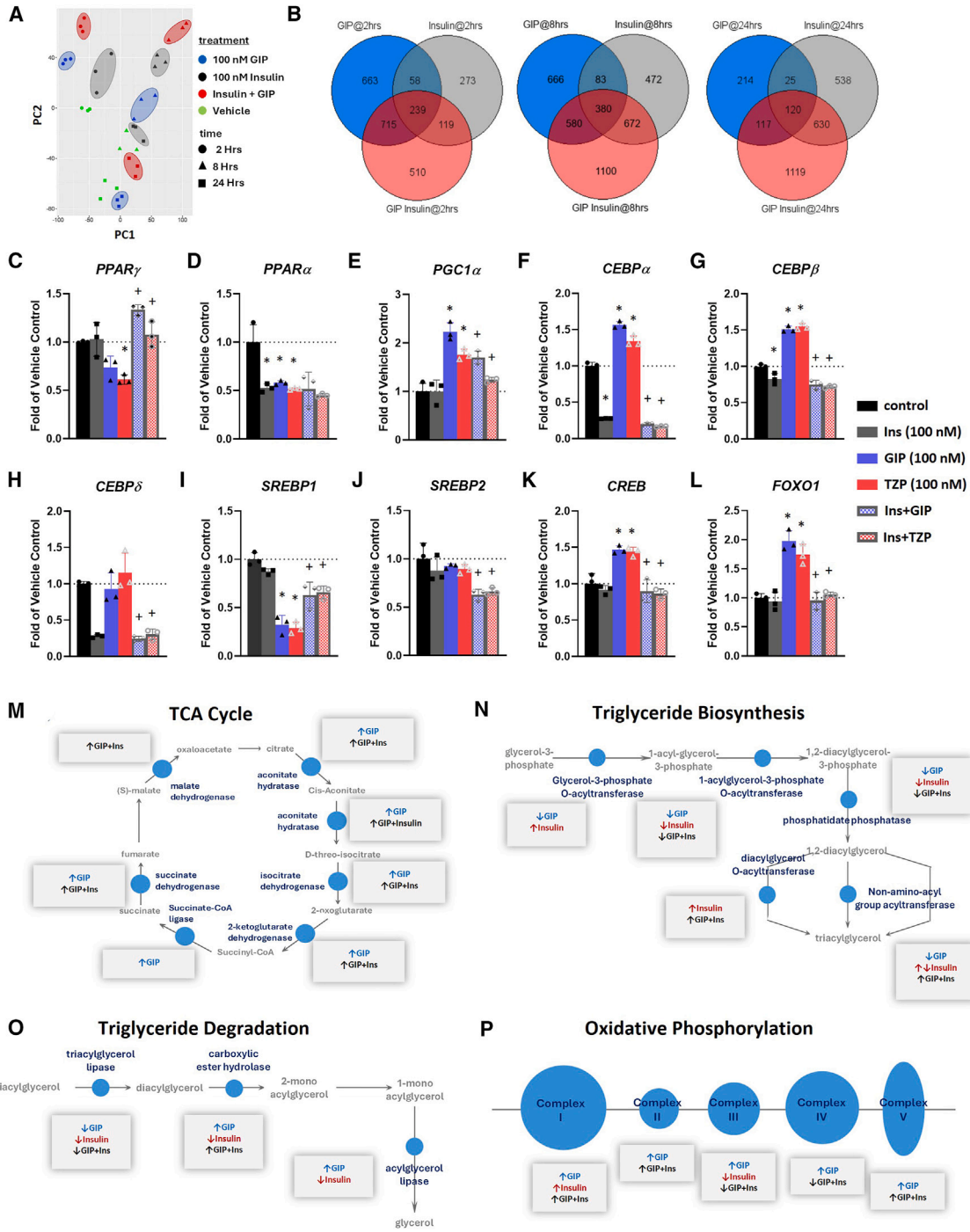

Figure 2. Tirzepatide and GIP regulate adipocyte transcriptional metabolic pathways both overlapping and distinct from insulin signaling

(A and B) Adipocytes treated with GIP, insulin, GIP + insulin, or vehicle for 2, 8, or 24 h ($n = 3$ replicates) followed by exome array and PCAs (A). mRNA expression levels with $p > 0.05$ and fold change </> 1.5 compared with vehicle represented in Venn diagram from all treatments (B).

(C–L) mRNA expression analysis of transcriptional regulators by Taqman (fold of control) of human adipocytes treated with control, insulin, GIP, tirzepatide, insulin + GIP, and insulin + tirzepatide for 8 h ($n = 3$ replicates).

(M–P) Canonical pathway analysis of exome array results with treatment directionality (up-/downregulation) using IPA on adipocytes treated with GIP, insulin, and insulin + GIP for 8 h ($n = 3$): TCA cycle (M), triglyceride biosynthesis (N), triglyceride degradation (O), and oxidative phosphorylation (P).

Data are represented as mean ± SEM. $^{*}p < 0.05$ (GIP or TZP versus vehicle), $^{+}p < 0.05$ (GIP versus insulin + GIP or TZP + insulin + TZP) by one-way ANOVA (C–L). TZP, tirzepatide.

See also Figures S2–S7.

Table 1. Key upstream regulators predicted by GIP and insulin treatment of adipocytes

Gene symbol	Protein name	Insulin		GIP		Insulin + GIP	
		Activation *Z* score	*p* value of overlap	Activation *Z* score	*p* value of overlap	Activation *Z* score	*p* value of overlap
CEBPα	CCAAT enhancer-binding protein alpha	−1.10	3.38E−4	0.26	6.70E−6	−0.81	1.12E−0.6
CEBPβ	CCAAT enhancer-binding protein beta	−0.27	6.39E−0.6	0.13	2.53E−13	−0.66	2.81E−7
CREB1	cyclic AMP-responsive element-binding protein 1	2.22	1.28E−10	2.53	5.08E−11	3.37	9.71E−14
FOXO1	forkhead box protein O1	−2.49	5.44E−13	−0.42	2.89E−20	−1.12	2.35E−14
PPARα	peroxisome proliferator-activated receptor alpha, PGC-1α	−1.39	6.19E−12	3.37	6.84E−15	0.58	1.85E−0.8
PPARδ	peroxisome proliferator-activated receptor beta or delta, PGC-1β/δ	–	–	2.63	3.97E−6	–	–
PPARγ	peroxisome proliferator-activated receptor gamma, PGC-1γ	0.68	7.01E−12	2.68	1.48E−18	1.31	2.11E−12
PPARGC1A	peroxisome proliferator-activated receptor gamma coactivator 1-alpha, PGC-1α	−0.10	4.84E−5	3.64	3.38E−15	1.36	3.94E−6
PPARGC1B	peroxisome proliferator-activated receptor gamma coactivator 1-beta, PGC-1β	2.07	3.39E−5	–	–	–	–
SREBF1	sterol regulatory element-binding transcription factor 1, SREBP1	4.38	3.23E−19	0.97	5.19E−12	2.04	9.63E−9
SREBF2	sterol regulatory element-binding transcription factor 2, SREBP2	4.67	3.07E−18	–	–	3.03	8.28E−6
TFAP2A	AP2, transcription factor AP-2 alpha	–	–	1.21	1.07E−0.5	1.83	3.55E−5

Upstream analysis (activation *Z* score and *p* value of overlap with differentially expressed mRNAs assessed using ingenuity pathway analysis) of adipocytes treated with GIP, insulin, and insulin + GIP for 8 h followed by exome array (n = 3 samples). Selected nuclear hormone receptors and transcription factors are shown.

To further explore mechanisms by which tirzepatide (GIPR agonism) enhanced glucose uptake in adipocytes in the presence of insulin, we assessed the activation of downstream components within the insulin signaling pathway by measuring Akt phosphorylation. Neither GIP nor tirzepatide increased Akt phosphorylation independent of insulin, but both GIPR agonists enhanced insulin-stimulated phosphorylation at the TORC2 and PDK phosphorylation sites of Akt (Figures 3C–3F), likely reflecting augmentation of insulin signaling. By contrast, insulin did not alter GIPR signaling as assessed by intracellular cAMP accumulation assays (Figure S8B).

We previously demonstrated that a LAGIPRA enhanced insulin sensitivity in mice after 2 weeks of chronic treatment, likely a combination of direct and indirect actions in adipose tissue.[24] Here, we investigated the direct, acute effect of GIPR agonism to enhance insulin-stimulated glucose uptake into adipose under hyperinsulinemic/euglycemic (HI/EG) clamp conditions in rats treated with streptozotocin to minimize potentially confounding effects of changes in endogenous insulin secretion. Native human GIP or vehicle was infused during the clamp (Figures 3G, S8C, and S8D). No significant change in glucose infusion rate (GIR; Figure 3H), skeletal muscle uptake (Figure 3I), or hepatic glucose production (Figure S8E) was observed with the acute infusion. However, adipose tissue glucose uptake was significantly increased with GIP infusion (Figure 3J), demonstrating a direct effect of GIP to enhance insulin-stimulated adipose tissue glucose uptake in rodents. Similar findings were observed when infusing an LAGIPRA with similar time-extension engineering to tirzepatide[25] in rodents during HI/EG clamp, demonstrating direct sensitization of insulin-stimulated glucose uptake into adipose (Figure S8F–S8J). These findings directly demonstrate the ability of tirzepatide to enhance glucose clearance into adipocytes and further suggest that GIP receptor activation can directly enhance insulin signaling to coordinately augment post-prandial glucose clearance into adipose tissue.

Tirzepatide and GIP regulate the metabolic fate of glucose

The influx of carbons from glucose uptake provides substrate for multiple metabolic pathways in adipocytes. We investigated whether this increased flux of glucose contributed to generation of glycerol or *de novo* lipogenesis (DNL, fatty acid synthesis). To evaluate whether the carbons in glucose contributed to generation of glycerol, we incubated adipocytes with heavy labeled glucose and conducted subsequent NMR analysis of lysates for carbon tracing. As expected, insulin increased the amount of labeled glycerol in adipocytes. Administration of GIP or tirzepatide both in the absence and presence of insulin produced even higher levels of labeled glycerol than insulin treatment alone. These data suggest GIPR agonism directly increases the conversion of glucose to glycerol (Figure 3K). These effects were not observed in unhydrolyzed samples (data not shown), indicating measurements reflected glycerol incorporated into triglycerides rather than free glycerol.

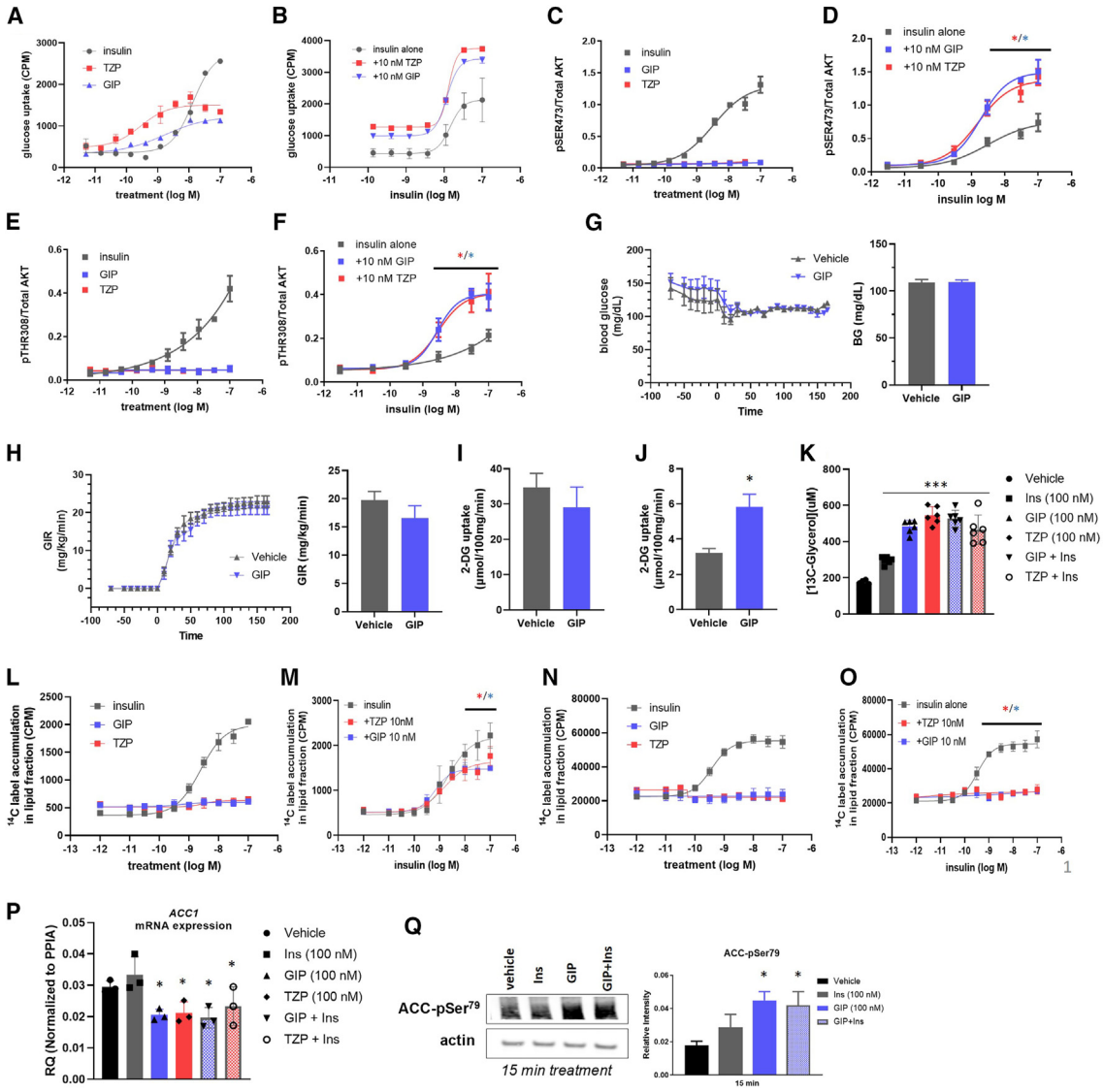

Figure 3. Tirzepatide regulates glucose metabolism similar to GIP both independently and coordinately with insulin in human adipocytes

(A and B) Radiolabeled glucose transport in differentiated human adipocytes to assess independent (A) and combined (B) regulation of glucose uptake by GIP, tirzepatide, and insulin (n = 2–3 replicates).

(C–F) Akt phosphorylation (n = 2–6 replicates) by ELISA at both Ser473 (C and D) and Thr308 (E and F) in response to GIP, tirzepatide, and insulin treatment both independently (C and E) and in combination (D and F).

(G–J) GIP or vehicle was infused during hyperinsulinemic/euglycemic clamp in streptozotocin-treated rats with subsequent 2-deoxy glucose infusion to determine tissue glucose uptake (n = 8 mice). Blood glucose during clamp (trace) and final 30 min average (G), glucose infusion rate (GIR) trace and final 30 min average (H), soleus muscle (I), and epididymal white adipose tissue (eWAT) (J) glucose uptake.

(K) Adipocytes were incubated with [^{13}C]glucose, and ^{13}C incorporation into glycerol was subsequently assessed by NMR on lysates from cells treated with GIP, tirzepatide, and insulin independently and in combination (n = 6 replicates).

(L–O) Adipocytes incubated with ^{14}C-glucose (J and K) or ^{14}C-acetate (L and M) and treated with GIP, tirzepatide, or insulin alone (L and N) or in combination (M and O), followed by analysis of ^{14}C incorporation into lysate (n = 2–6 replicates).

(P and Q) Adipocytes treated with GIP, tirzepatide, insulin, and combinations followed by mRNA analysis for *ACC1* expression by Taqman (P). Adipocytes treated with vehicle, insulin, and GIP for 15 min followed by western blot for Ser^{79}, an inactivating residue on ACC (n = 3 replicates) (Q).

Data are represented as mean ± SEM. *p < 0.05, **p < 0.01, ***p < 0.001 by two-way ANOVA (D, F, M, and O) and one-way ANOVA (I–K).

TZP, tirzepatide.

See also Figure S8.

To determine whether carbons from increased glucose flux into adipocytes were contributing to fatty acid synthesis, we incubated cells with ^{14}C-glucose or ^{14}C-acetate with carbon tracing into the lipid fraction of the cells to examine regulation of DNL or fatty acid synthesis. We included the use of labeled acetate in addition to labeled glucose in these assays since acetate

contributes readily to the formation of new fatty acids and serves as a good model for DNL/fatty acid synthesis. Unlike insulin, neither GIP nor TZP directly increased DNL (Figures 3L–3N). Notably, both tirzepatide and GIP reduced insulin-stimulated DNL from both glucose and acetate (Figures 3M and 3O). Consistent with a reduced rate of DNL, tirzepatide and GIP decreased ACC mRNA expression levels of *ACC1*, a rate-limiting enzyme for DNL, compared with insulin, and increased phosphorylation of an inactivating residue on ACC (ACC-pSer[79]) (Figures 3P and 3Q). These findings suggest that activation of GIPR signaling by tirzepatide in adipocytes may restrict fatty acid synthesis from glucose via inhibition of ACC activity in favor of increasing generation of glycerol aiding in the storage of postprandial dietary lipids.

Tirzepatide and GIP improve lipid clearance into adipocytes

Hierarchal clustering of gene sets associated with lipid metabolism curated using IPA and KEGG pathways demonstrated both similar and distinct differentially regulated mRNA expression patterns when comparing effects of GIP and insulin administration expression patterns comparing GIP and insulin treatments (Figures S9A and S9B). To compare tirzepatide and IR regulation of lipid clearance into adipocytes, we first examined regulation of lipoprotein lipase (LPL) expression and activity as a key mediator of the uptake of lipoprotein triglyceride-derived fatty acids into cells. Similar to insulin, tirzepatide and GIP both dose-dependently increased mRNA expression, secretion, and activity of LPL (Figures 4A–4C). This suggests tirzepatide may indeed increase the extracellular hydrolysis of lipoprotein-derived triglyceride in adipose tissue, a critical step in clearing dietary triglycerides into adipocytes for storage. Next, we modeled fatty acid uptake to determine whether tirzepatide/GIPR agonism could enhance fatty acid transport into adipocytes. Tirzepatide and GIP stimulated an increase in fatty acid uptake in a manner similar to insulin (Figure 4D) and demonstrated an additive effect when combined with insulin (Figures 4E and 4F). These findings suggest that chronic GIPR agonists, including tirzepatide, can enhance dietary lipid clearance into adipocytes, working in concert with insulin to hydrolyze and transport lipid molecules into adipocytes.

GIPR agonism *in vivo* improves dietary lipid clearance into adipose without increasing adiposity

The adipocyte findings here suggest tirzepatide via its GIPR agonism may improve lipid clearance into adipocytes, providing better post-prandial lipid partitioning and potentially long-term benefits in lowering plasma triglyceride levels. To study postprandial regulation of lipid partitioning, we treated mice with an LAGIPRA 1 day before oral lipid challenge. We employed the GIPR monoagonist to study the GIP component of tirzepatide as the GLP-1R agonist component of tirzepatide potently delays gastric emptying complicating interpretation of an oral lipid challenge. LAGIPRA dose-dependently reduced the triglyceride excursion post-lipid gavage (Figure 4G). The reduction in triglyceride excursion was not a function of reduced gastric emptying as reflected by measures of stomach weight (Figure 4I). This effect of LAGIPRA was blocked by treatment with tyloxapol, an inhibitor of plasma lipolytic activity (Figure 4H), suggesting the lipid-clearing effects of LAGIPRA are likely to be partially dependent on LPL. Infusion of TRL-like particles containing glycerol tri [^{3}H]oleate demonstrated GIPR but not GLP-1R agonism increased [^{3}H]oleate partitioning into adipose. Treating mice 1 day prior with LAGIPRA increased [^{3}H]-label accumulation in white adipose tissue, whereas a long-acting GLP-1R agonist[26] had no effect (Figure 4J). After 4 days of dosing with LAGIPRA, serum triglycerides were reduced, both in the dark photoperiod when mice are feeding and in the light photoperiod when mice are fasting (Figures 4K and 4L). These data suggest the long-acting GIPR agonism component of tirzepatide likely increases clearance of dietary lipid into adipose tissue that may contribute to the clinically observed decreases in serum triglyceride levels.

To test whether increasing the ability of adipocytes to clear and store macronutrients via chronic GIPR agonism could potentially lead to increased adiposity, we treated diet-induced obese (DIO) mice with a high dose of LAGIPRA for 2 weeks. LAGIPRA was weight neutral (Figure 4M), with no increase in adiposity (Figure 4N). Serum triglycerides were reduced, consistent with the more acute studies, demonstrating a conserved effect of the GIPR agonist to regulate lipid metabolism with chronic treatment (Figure 4O). Light photoperiod (fasted) plasma glucose was reduced (Figure 4P) with no change in fasting insulin levels (Figure 4Q). These findings demonstrate that chronic GIPR agonism does not increase adiposity or result in weight gain but does improve serum triglyceride levels while improving glycemic control.

Tirzepatide enhances adipocyte lipid efflux when insulin levels are low

To regulate whole-body lipid homeostasis, adipose tissue plays a pivotal role in releasing stored lipid during periods of low plasma nutrient load and low insulin levels. To better understand whether tirzepatide regulates lipid efflux from adipocytes, we treated adipocytes with GIP, tirzepatide, or insulin and measured glycerol release from cells as a function of lipolysis. Both tirzepatide and GIP stimulated lipolytic function, whereas insulin suppressed lipolysis (Figure 5A). Interestingly, the lipolytic function of GIP or tirzepatide was fully suppressed with insulin treatment (Figure 5B). Expression and post-translational modification of lipolytic enzymes were consistent with this counter-regulation. Both GIP and tirzepatide increased mRNA expression levels of key lipolytic enzymes *HSL* and *FABP4*, an effect that was suppressed by insulin (Figure 5C). Additionally, GIP increased phosphorylation of HSL at a key activating site (Figure 5D). These findings demonstrate tirzepatide/GIPR agonism can regulate human adipocyte lipolysis in an insulin-dependent manner.

Enhancing lipid efflux during periods of nutrient depletion should enable greater lipid mobilization from adipose during energy demand and subsequent increased lipid oxidation. To investigate whether the dual agonist components of tirzepatide function in this manner, we treated DIO mice with LAGIPRA, the GLP-1R monoagonist semaglutide, and combination for 72 h and measured the respiratory exchange ratio (RER) to assess changes in lipid/carbohydrate utilization. LAGIPRA, semaglutide, or combination significantly reduced food consumption compared with vehicle, with the combination producing slightly greater reductions in caloric intake (Figure 5E). Associated with reductions in food intake, treatment with LAGIPRA or

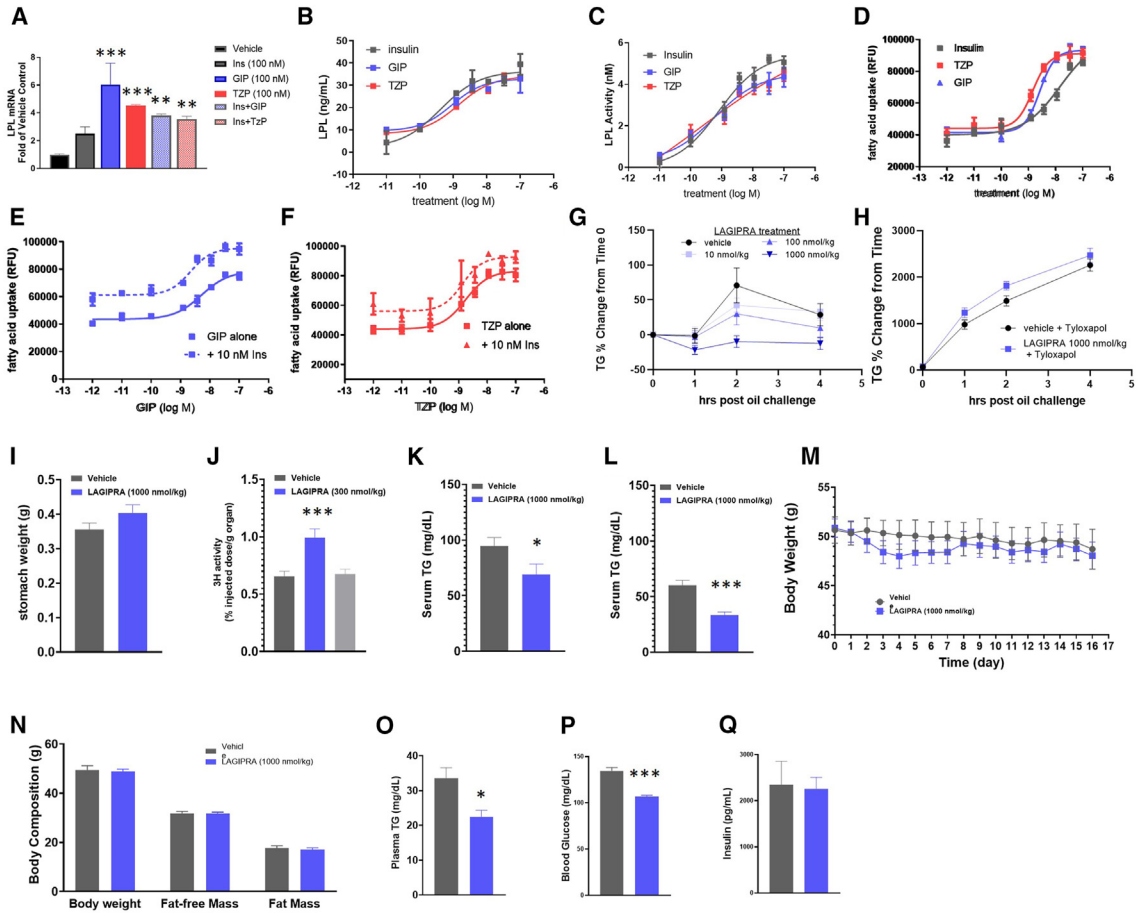

Figure 4. Tirzepatide and long-acting GIPR agonism regulate lipid clearance into adipocytes, reducing plasma triglycerides independent of changes in body composition

(A–C) Adipocytes were treated with GIP, tirzepatide, or insulin, and in combination (n = 3 replicates), followed by mRNA analysis for *LPL* (A). Conditioned media from adipocytes treated with GIP, tirzepatide, or insulin (n = 3 replicates) were assessed for LPL secretion by ELISA (B) and LPL activity (C).

(D–F) Adipocytes were treated with GIP, tirzepatide, or insulin alone (n = 3) (D) and in combination (n = 3 replicates) (E and F) and incubated with fluorescently labeled fatty acid substrate followed by analysis for fatty acid uptake.

(G–I) Mice dosed with LAGIPRA 1 day prior to corn oil challenge followed by assessment of serum triglyceride excursion over 4 h without (n = 9 mice; G) and with (n = 12 mice; H) the LPL inhibitor tyloxapol. Stomach weights measured for vehicle and 1,000 nmol LAGIPRA treatment at terminal bleed (n = 12 mice) (I).

(J) Synthetic glycerol tri[^{3}H]oleate-labeled TRL-like particles were intravenously (i.v.) infused into mice following overnight treatment with LAGIPRA or LAGLP-1RA followed by analysis of [^{3}H]oleate uptake by gonadal WAT (n = 10 mice).

(K and L) Serum triglyceride levels in mice dosed daily for 3 days with LAGIP; after final dose both dark cycle (feeding) (K) and light cycle (fasting) (K) (n = 10 mice).

(M–Q) DIO mice (n = 5 mice) were treated for 16 days with LAGIPRA (n = 5) and assessed for body weight (M). At 16 days, body composition assessed by qNMR (N). Plasma triglyceride, glucose, and insulin were measured at day 16 (O–Q). Statistical tests included unpaired Student's t test (vehicle versus treatment: D–F, I, and J).

Data are represented as mean ± SEM. *p < 0.05, **p < 0.01, ***p < 0.001 by one-way ANOVA (A and J), Student's t test (I K, L, and O–Q), or two-way ANOVA (N). TZP, tirzepatide.

See also Figure S9.

semaglutide demonstrated a minimal reduction in RER. However, the addition of LAGIPRA to semaglutide resulted in a pronounced reduction in RER (Figures 5F and 5G) despite producing minimal further reduction in food intake compared with semaglutide alone. These findings suggest addition of GIPR agonism to GLP-1R agonism may increase whole-body oxidation of lipid macronutrients via enhanced lipid release from adipose tissue during periods of negative caloric balance when availability and utilization of stored energy becomes important to sustain normal tissue functions. As the anorectic effect of GLP-1R agonism drives the need for utilization of stored energy macronutrients, the addition of GIPR agonism improves the ability to satisfy this demand by enhancing liberation of stored lipids from adipose. This framework identifies a potential additional mechanism for greater reductions in fat mass observed with tirzepatide versus GLP-1R monoagonists.[23,27]

DISCUSSION

The long-acting dual GIPR/GLP-1R agonist tirzepatide has demonstrated greater weight reduction, improved HbA1c, and triglyceride reduction compared with selective GLP-1R agonists

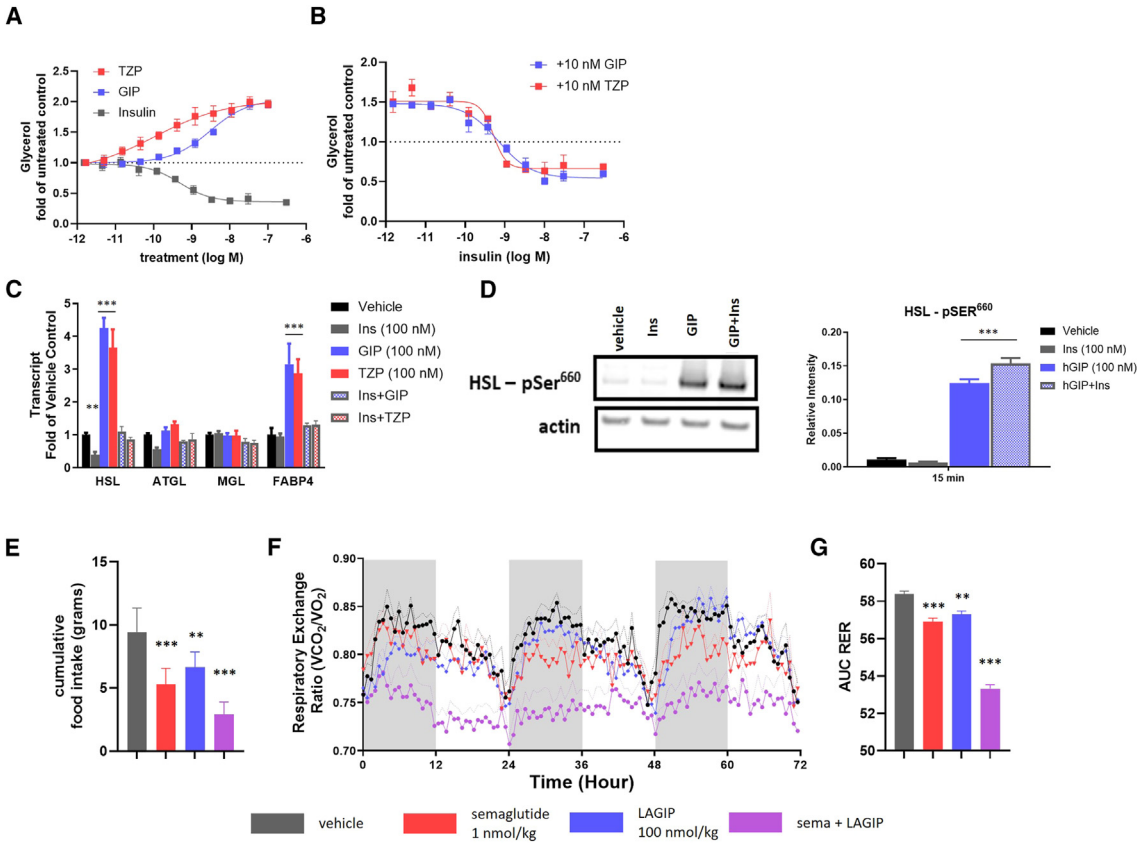

Figure 5. Tirzepatide and long-acting GIPR agonism regulate lipid efflux from adipocytes in an insulin-dependent manner and improve lipid oxidation associated with reduced food intake

(A–D) Adipocytes were treated with GIP, tirzepatide, or insulin alone (A) and in combination (B) followed by analysis of glycerol accumulation in media (n = 3 replicates). Adipocytes treated with GIP, tirzepatide, or insulin and combinations followed by mRNA analysis for *HSL*, *ATGL*, *MGL*, and *FABP4* (C). Western blot analysis for pSer^{660}, an activating residue, on HSL following a 15-min treatment with insulin, GIP, and combination (n = 3 replicates) (D).

(E–G) DIO mice (n = 5–6) were treated with vehicle, semaglutide, LAGIPRA, or combination daily for 3 days in respiratory chambers for indirect calorimetry. Cumulative food intake (E) and RER (F and G).

Data are represented as mean ± SEM. *p < 0.05, **p < 0.01, ***p < 0.001 by two-way ANOVA (C) or one-way ANOVA (D, E, and G).

TZP, tirzepatide.

in individuals with T2D.[2–6] Although the mechanisms by which GLP-1R agonists provide beneficial pharmacology have been widely studied,[28] our observations now provide evidence for GIPR-regulated adipose tissue-specific effects contributing to the salutary effects of tirzepatide. Here, we demonstrate the ability of long-acting GIPR agonism to regulate adipocyte carbohydrate and lipid metabolism. Based on these findings, we propose a model whereby long-acting GIPR agonism modulates both storage and release of high-energy macronutrients differentially in the fasted and fed states, such that in the fasting state (low insulin levels) energy release and in the fed state (high insulin levels) energy storage is stimulated. These findings help to better elucidate the potential benefits of combining long-acting GIPR agonism with GLP-1R agonism.

In this study, we demonstrated the ability of tirzepatide to directly regulate adipocyte function. Recent findings using mouse genetic models and cellular genomic techniques suggested that GIPR may be predominantly localized to non-adipocyte cell types within white adipose tissue.[15,16] Here, we demonstrate binding of GIPR targeting agonists (GIPRA-FL, TZP-FL) but not GLP-1R monoagonist (Ex4-FL) broadly to adipocytes within whole mouse and human adipose tissue, expression of GIPR mRNA via RNAscope in adipocytes from human and mouse adipose, GIPR mRNA expression, signaling, and function in isolated human and mouse adipocytes, and GIPR gene expression and signaling with tirzepatide and GIP in differentiated human adipocytes. Additionally, and consistent with the recent report, we found GIPR expressed in the non-adipocyte fraction and GIPR targeting peptides bound along the vasculature, suggesting some GIPR expression in the perivascular niche within adipose tissue. The results presented here provide evidence for broad expression of functionally active GIPR on adipocytes in human and mouse adipose tissue and for GIPR-mediated regulation of adipocyte metabolism, highlighting adipose tissue as an important target for GIPR agonists.

These findings confirm the unique ability of GIPR/GLP-1R agonists to directly regulate adipose tissue function and illustrate modulation of adipocyte function as an important mechanistic target of tirzepatide. Of particular interest is the temporal context in which tirzepatide engages adipocyte GIPR compared with

native/endogenous GIPR signaling. Endogenous GIP secretion during a meal or glucose challenge results in patterns of plasma GIP excursions similar to that of insulin[29,30] enabling simultaneous signaling to adipocytes via activation of the IR as well as the GIP receptor. As such, most studies concerning GIP regulation of adipocyte function have focused on explaining endogenous post-prandial actions in the context of insulin signaling. However, tirzepatide was engineered as a long-acting agonist, with clinical pharmacokinetics supporting engagement of GIPR in both the post-prandial and post-absorptive states.[23] Thus, to explore the effects of long-acting GIPR agonism on regulation of adipocyte function, we assessed the impact of GIPR signaling in the presence but also absence of insulin. At a high level, transcriptomics demonstrated GIPR agonism independent of insulin broadly regulates adipocyte function by directly modulating expression of key metabolic transcription factors and nuclear hormone receptors (PPARs, PGC1α, SREBPs, and FOXO1). Consistent with this, GIP influenced transcriptional regulation of carbohydrate (TCA cycle) and lipid (triglyceride metabolism) metabolic pathways and cellular energy balance (oxidative phosphorylation) with similar or greater pathway saturation than insulin. These findings suggest chronic GIPR agonism can be a potent and insulin-independent regulator of adipocyte nutrient metabolism, in addition to enhancing insulin action in adipocytes. Modulation of mRNA expression for key adipocyte metabolism regulators and canonical metabolic pathways by GIP is counter regulated in the presence and absence of insulin. The potential for LAGIPRAs to differentially regulate adipocyte metabolism in the fed and fasted states is particularly intriguing. Hence, follow-up functional studies for lipid and carbohydrate metabolism were performed to better understand metabolic pathways coregulated and counter regulated by GIP and insulin.

GIP has been shown to enhance insulin sensitivity and glucose uptake in adipocytes,[31,32] suggesting an important role for endogenous GIP in post-prandial glucose clearance. Consistent with these reports, our studies demonstrate tirzepatide directly increases adipocyte glucose uptake and enhances both insulin signaling and insulin-stimulated glucose uptake. Clinical GIP infusions during hyperglycemic clamp have demonstrated enhanced glucose clearance into adipose tissue[33]; however, it is difficult to dissociate the direct effects of GIP on adipose glucose metabolism from elevated insulin/C-peptide observed during the clamp with GIP infusion. The HI/EG clamp studies presented here in streptozotocin-treated rats demonstrate a clear GIP-dependent increase in adipose tissue glucose uptake. Of interest, this acute infusion was not sufficient to alter GIR, though we previously published the weight-independent, whole-body insulin-sensitizing effects of chronic, long-acting GIPR agonism during which GIP enhanced adipose tissue glucose uptake.[24] This suggests GIP indeed has a direct action to enhance post-prandial glucose clearance into adipose tissue during acute and chronic dosing, though whole-body insulin-sensitizing effects require longer-term treatment. These direct actions of tirzepatide on adipocytes to enhance insulin signaling and glucose uptake are in addition to its incretin function[23] via engagement of GIPR and GLP-1R on pancreatic beta cells. As such, the addition of GIPR agonism to GLP-1R agonism provides multiple mechanisms for improving post-prandial glucose control potentiating both insulin secretion from beta cells and insulin action through glucose disposal into adipose. This added benefit of GIPR agonism to enhance adipocyte insulin signaling and glucose uptake may indeed be a key contributor to clinical improvements in glycemic control and insulin sensitivity observed in subjects with T2D treated with tirzepatide as compared with those administered a selective GLP-1R agonist.[4,5]

Our studies also provide more insight into the metabolic fate of increased glucose uptake into adipocytes stimulated by GIPR agonism. DNL in adipocytes or the conversion of excessive carbohydrates to fatty acids has been shown as an important metabolic pathway associated with insulin sensitivity.[34,35] Additionally, carbohydrate flux into adipocytes contributes to glycerogenesis. This is an important metabolic pathway for excess glucose disposal into white adipose tissue,[36] and also contributes to the glycerol pool available for generation of glycerol 3-phosphate and subsequent triglyceride synthesis.[37] Our findings show GIPR agonism biases the contribution of glucose carbons away from DNL (reducing insulin-stimulated DNL potentially via modulation of ACC1) and toward the generation of glycerol. This proposes that GIPR agonism, in tandem with insulin in the fed state, enhances the capacity for storage of dietary free fatty acid (FFA)/triglyceride as intracellular triglyceride by increasing the available glycerol pool as opposed to the synthesis of new FFAs. Although reduced subcutaneous adipose DNL has been associated with insulin resistance, long-acting GIPR agonism has been shown to increase whole-body and adipose insulin sensitivity in mice,[24] suggesting any potential reductions in DNL from GIPR agonists do not induce insulin resistance. Further, clinical improvements in HbA1c and insulin sensitivity are observed in T2D subjects treated with tirzepatide,[5,38] suggesting GIPR agonism in the context of GLP-1R agonism does not potentiate insulin resistance but rather enhances whole-body insulin sensitivity.

Adipose is the key tissue for storage of excess dietary lipid, and failure or reduced capacity to do so can result in dietary spillover and subsequent elevation of serum-FFAs and triglycerides and unwanted ectopic lipid accumulation in non-adipose tissues.[39,40] Our findings suggest tirzepatide enhances partitioning of dietary lipids into adipose tissue via sustained GIPR agonism. Clearance of triglycerides into adipose first requires LPL-mediated hydrolysis into glycerol and FFAs followed by uptake of the liberated fatty acids into adipocytes.[41] Defects in LPL-mediated plasma triglyceride clearance are associated with insulin resistance and dyslipidemia,[42] and therapeutic intervention to improve this would be of benefit.[43] GIP treatment of adipocytes has been shown to increase LPL production and activity[44,45] and clinical GIP infusions have resulted in increased triglyceride-derived fatty acid uptake into adipose tissue.[33,46] The activity of tirzepatide in adipocytes is consistent with this increasing human adipocyte LPL expression, secretion, and function, similar to GIP and insulin, while also increasing FFA uptake in an additive manner with insulin. These findings suggest the ability for tirzepatide to both enhance extracellular hydrolysis of dietary lipid in adipose tissue and subsequently increase uptake of liberated fatty acids via GIPR agonism in adipocytes, resulting in improved post-prandial lipid clearance into adipose. Indeed, treatment with LAGIPRA in our models decreased plasma triglyceride excursions after oral lipid challenge, an effect that appears dependent upon LPL in adipocytes with GIPR, but not GLP-1R,

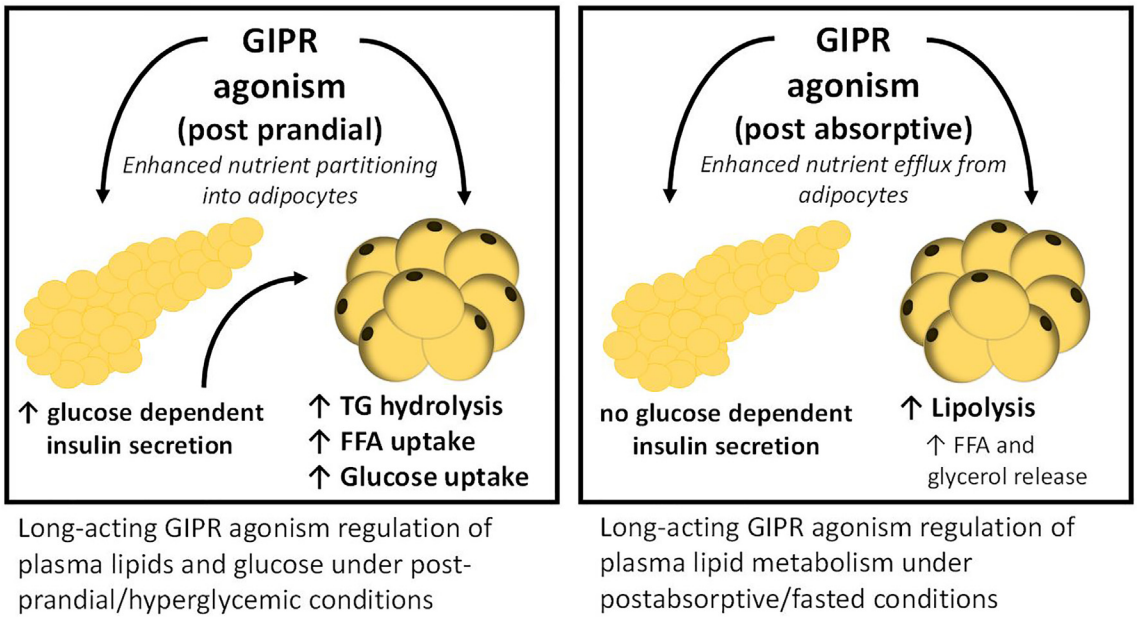

Figure 6. Proposed model of the fasted and fed effects of long-acting GIPR agonism by tirzepatide regulating adipose tissue function

agonism-enhancing adipose tissue triglyceride-derived fatty acid uptake. Improvements in post-prandial lipid clearance into adipose represent an overall improvement in lipid homeostasis and should result in reduced triglycerides, an effect we observed with LAGIPRA both during feeding and fasting periods with acute dosing (4 days of treatment) and chronic dosing (14 days of treatment). These findings provide mechanistic insight into the clinically observed benefit of tirzepatide compared with GLP-1R monoagonists to reduce serum triglycerides and elevate LPL.[3] Additionally, these direct actions of tirzepatide to improve adipocyte post-prandial macronutrient clearance/storage in adipocytes may serve to reduce ectopic lipid deposition potentially contributing to the observed preclinical and clinical improvements in insulin sensitivity after chronic treatment.[24] Although it has been suggested that potential action of GIP to enhance triglyceride storage in adipose may exacerbate obesity and insulin resistance,[46] we found chronic dosing in mice with LAGIPRA to be weight neutral, not increasing fat mass, and improving glycemic control. Further, tirzepatide treatment in T2D subjects reduced bodyweight and waist circumference compared with active GLP-1R monoagonist.[4,5]

In addition to the storage of macronutrients, adipose tissue is also responsible for the release of stored lipid during the post-absorptive state. Adipocytes achieve this via lipolytic breakdown of stored triglyceride and subsequent release of glycerol and FFAs.[47] GIP has been shown to regulate intracellular lipolytic function *in vitro*[17,18] and clinical GIP infusions have resulted in increased plasma glycerol and FFAs under various conditions,[48,49] suggesting GIPR agonism may regulate the efflux of stored lipid in addition to regulating influx of lipid in adipocytes. Consistent with this, we demonstrated tirzepatide stimulates lipolysis in human adipocytes while increasing expression and activation state of HSL, a key enzyme involved in the lipolytic breakdown of stored triglycerides. Our findings, however, suggest the lipolytic effect of chronic GIPR agonism would be limited to periods of fasting, as tirzepatide-stimulated lipolysis was inhibited by co-treatment with insulin. This modeled suppression of lipolytic function during the fed state is important as post-prandial release of FFAs is associated with insulin resistance.[50] This effect of long-acting GIPR agonism to potentially enhance release of stored lipid only during periods of energy demand becomes particularly interesting in the context GLP-1R agonism. Interestingly, GIPR agonism synergistically enhances GLP-1R weight loss in mice[51] through incompletely understood mechanisms. The studies presented here showed a dramatic reduction in RER associated with reduced food intake when adding GIP to GLP-1 in DIO mice, suggesting a greater oxidation of stored lipid with dual agonism compared with GLP-1R monoagonism alone. This proposes a mechanism whereby increased post-absorptive adipocyte lipolysis from GIPR agonism may contribute to the enhanced weight loss by more readily mobilizing lipid stores from adipose in overweight or obese individuals during negative caloric balance. Future *in vivo* and clinical studies measuring energy expenditure and lipid oxidation with defined caloric intake would be of interest to better evaluate this concept. Collectively, our findings suggest GIPR-mediated actions on adipocytes that likely contribute to superior weight loss in clinical studies with tirzepatide compared with GLP-1R monoagonists.[2,4]

Based on the findings presented here, we propose a model by which the long-acting GIPR agonism of tirzepatide augments both fed and fasted macronutrient partitioning in adipose (Figure 6). Working with insulin in the fed state, tirzepatide improves extracellular hydrolysis of dietary triglycerides and subsequent uptake of liberated fatty acids while also increasing glucose uptake and conversion to glycerol, supporting glucose clearance and triglyceride synthesis within adipocytes. When insulin levels are reduced in states of fasting and increased energy demand, tirzepatide enhances energy release from adipocytes via

lipolysis, supporting energy when plasma nutrient levels are depleted. This model proposes a route by which GIPR agonism in adipose adds to the GLP-1-mediated effects on glycemia and body weight by further improving glycemic control and insulin sensitivity, reducing serum triglycerides, and decreasing body weight and adiposity.

Limitations of the study

We recognize that the actions of tirzepatide and GIPR agonism in adipose are mediated in tandem with regulation of additional cell types and organ systems. Of note, engagement of GIPR and GLP-1R by tirzepatide in the endocrine pancreas leads to alterations in insulin secretion affecting nutrient metabolism in multiple tissues including adipose. Additionally, central regulation of appetite by tirzepatide alters both the level and composition of carbohydrates and lipids in plasma. Although we have demonstrated engagement and regulation of adipocytes and adipose tissue function *in vitro* and *in vivo*, the actions of tirzepatide via engagement of its target receptors in various tissues provide an additional indirect regulation of adipose tissue metabolism. Further, multiple cell types in adipose, in addition to the adipocyte, have been shown to express GIPR and could provide additional opportunities for GIP signaling to contribute to the regulation of adipose tissue function and energy balance.[15,52,53] Future efforts to further dissect contribution of these indirect and direct actions will be of interest as additional multi-agonists targeting the GIPR emerge.

Additionally, clinical translation for LAGIPRA regulation of nutrient partitioning has been challenging as long-acting GIPR monoagonist tool molecules have not been unavailable. However, clinical investigation of such molecules has recently been reported (ClinicalTrials.gov, Identifier NCT04923269; ClinicalTrials.gov, Identifier NCT05144984; ClinicalTrials.gov, Identifier NCT04586907).[54–56] Initial reports suggest GIPR agonism indeed provides metabolic benefit[57] consistent with mechanisms presented here. Future clinical studies should ultimately help better elucidate potential mechanistic benefits of long-acting GIPR agonism in the context of GLP-1R agonism.

STAR★METHODS

Detailed methods are provided in the online version of this paper and include the following:

- KEY RESOURCES TABLE
- RESOURCE AVAILABILITY
  - Lead contact
  - Materials availability
  - Data and code availability
- EXPERIMENTAL MODEL AND STUDY PARTICIPANT DETAILS
- METHOD DETAILS
  - Adipocyte culture and differentiation
  - Glucose Uptake
  - Lipogenesis
  - Lipolysis
  - Protein Electrophoresis and Western Blot
  - RNA Isolation and cDNA synthesis
  - RT PCR
  - Taqman Probes Used
  - cAMP Assay
  - Total and phospho-AKT Assay
  - Fatty Acid uptake Assay
  - LPL Assay
  - ^{13}C-Glycerol measurement by NMR
  - Exome Array Analysis
  - Trace fluorescently labeled molecules
  - In Vivo Experiments
  - Body Weight and Composition in Diet-induced Obese Mice
  - Acute Oral Lipid Challenge in Lean Mice
  - Triglycerides Assessment after Semi-Chronic Repeat Dose in Lean Mice
  - Organ uptake of triglyceride-rich lipoprotein-mimicking particles in Lean Mice
  - Calorimetry in DIO mice
  - Hyperinsulinemic/euglycemic clamp studies

SUPPLEMENTAL INFORMATION

Supplemental information can be found online at https://doi.org/10.1016/j.cmet.2024.05.010.

ACKNOWLEDGMENTS

We thank Robin van Eenige for setting up, performing, and analyzing the *in vivo* experiments performed at the Leiden University Medical Center, Leiden, the Netherlands. Funding for this study was provided by Eli Lilly and Company.

AUTHOR CONTRIBUTIONS

Conceptualization, W.R., A.R., P.C.N.R., T.C., and M.K.T.; methodology, W.R., A.R., E.A., M.E.C., G.V., Y.L., S.K., and T.C.; formal analysis, W.R., A.R., E.A., M.E.C., G.V., T.P.B., E.B., L.S.O., M.A.B., A.K.A., X.R., Y.L., H.H., D.L.K., S.W., A.K.H., J.L.F., A.S.E., H.S.B., G.S.G., S.K., P.C.N.R., and T.C.; resources, E.A., R.A.B., and S.K.; data curation, G.V., Y.L., and S.K.; writing – original draft, W.R., A.R., and M.K.T.; writing – review & editing, W.R., A.R., P.C.N.R., S.K., T.C., and M.K.T.; visualization, W.R., E.A., M.E.C., G.V., L.S.O., S.K., T.C., and M.K.T.; supervision, W.R., M.E.C., P.C.N.R., and T.C.; project administration, W.R.

DECLARATION OF INTERESTS

A.R., E.A., M.E.C., G.V., T.P.B., X.R., E.B., L.S.O., M.A.B., A.K.A., Y.L., H.H., D.L.K., S.W., A.K.H., J.L.F., R.A.B., A.S.E., H.S.B., G.S.G., T.C., M.K.T., and W.R. are employees and shareholders at Eli Lilly and Company. P.C.N.R. is supported by the Cardiovascular Research Netherlands for the GENIUS-2 project "Generating the best evidence-based pharmaceutical targets for atherosclerosis" (CVON 2017-20).

Received: October 2, 2023
Revised: February 20, 2024
Accepted: May 21, 2024
Published: June 14, 2024; corrected online: June 25, 2024

REFERENCES

1. International Diabetes Federation (2021). IDF Diabetes Atlas, Tenth Edition (International Diabetes Federation). https://www.diabetesatlas.org.
2. Frias, J.P., Nauck, M.A., Van, J., Kutner, M.E., Cui, X., Benson, C., Urva, S., Gimeno, R.E., Milicevic, Z., Robins, D., et al. (2018). Efficacy and safety of LY3298176, a novel dual gip and glp-1 receptor agonist, in patients with type 2 diabetes: a randomised, placebo-controlled and active comparator-controlled phase 2 trial. Lancet *392*, 2180–2193. https://doi.org/10.1016/S0140-6736(18)32260-8.
3. Wilson, J.M., Nikooienejad, A., Robins, D.A., Roell, W.C., Riesmeyer, J.S., Haupt, A., Duffin, K.L., Taskinen, M.R., and Ruotolo, G. (2020). The dual glucose-dependent insulinotropic peptide and glucagon-like peptide-1 receptor agonist, tirzepatide, improves lipoprotein biomarkers associated with insulin resistance and cardiovascular risk in patients with type 2 diabetes. Diabetes Obes. Metab. *22*, 2451–2459. https://doi.org/10.1111/dom.14174.

4. Frías, J.P., Davies, M.J., Rosenstock, J., Pérez Manghi, F.C., Fernández Landó, L., Bergman, B.K., Liu, B., Cui, X., and Brown, K.; SURPASS-2 Investigators (2021). Tirzepatide versus semaglutide once weekly in patients with type 2 diabetes. N. Engl. J. Med. *385*, 503–515. https://doi.org/10.1056/NEJMoa2107519.

5. Heise, T., Mari, A., DeVries, J.H., Urva, S., Li, J., Pratt, E.J., Coskun, T., Thomas, M.K., Mather, K.J., Haupt, A., et al. (2022). Effects of subcutaneous tirzepatide versus placebo or semaglutide on pancreatic islet function and insulin sensitivity in adults with type 2 diabetes: a multicentre, randomised, double-blind, parallel-arm, phase 1 clinical trial. Lancet Diabetes Endocrinol. *10*, 418–429. https://doi.org/10.1016/S2213-8587(22)00085-7.

6. Jastreboff, A.M., Aronne, L.J., Ahmad, N.N., Wharton, S., Connery, L., Alves, B., Kiyosue, A., Zhang, S., Liu, B., Bunck, M.C., et al. (2022). Tirzepatide once weekly for the treatment of obesity. N. Engl. J. Med. *387*, 205–216. https://doi.org/10.1056/NEJMoa2206038.

7. Nauck, M.A., Bartels, E., Orskov, C., Ebert, R., and Creutzfeldt, W. (1993). Additive insulinotropic effects of exogenous synthetic human gastric inhibitory polypeptide and glucagon-like peptide-1-(7–36) amide infused at near-physiological insulinotropic hormone and glucose concentrations. J. Clin. Endocrinol. Metab. *76*, 912–917. https://doi.org/10.1210/jcem.76.4.8473405.

8. Gasbjerg, L.S., Helsted, M.M., Hartmann, B., Jensen, M.H., Gabe, M.B.N., Sparre-Ulrich, A.H., Veedfald, S., Stensen, S., Lanng, A.R., Bergmann, N.C., et al. (2019). Separate and combined glucometabolic effects of endogenous glucose-dependent insulinotropic polypeptide and glucagon-like peptide 1 in healthy individuals. Diabetes *68*, 906–917. https://doi.org/10.2337/db18-1123.

9. Adriaenssens, A.E., Biggs, E.K., Darwish, T., Tadross, J., Sukthankar, T., Girish, M., Polex-Wolf, J., Lam, B.Y., Zvetkova, I., Pan, W., et al. (2019). Glucose-dependent insulinotropic polypeptide receptor-expressing cells in the hypothalamus regulate food intake. Cell Metab. *30*, 987–996.e6. https://doi.org/10.1016/j.cmet.2019.07.013.

10. Gabery, S., Salinas, C.G., Paulsen, S.J., Ahnfelt-Rønne, J., Alanentalo, T., Baquero, A.F., Buckley, S.T., Farkas, E., Fekete, C., Frederiksen, K.S., et al. (2020). Semaglutide lowers body weight in rodents via distributed neural pathways. JCI Insight *5*, e133429. https://doi.org/10.1172/jci.insight.133429.

11. Hansen, H.H., Perens, J., Roostalu, U., Skytte, J.L., Salinas, C.G., Barkholt, P., Thorbek, D.D., Rigbolt, K.T.G., Vrang, N., Jelsing, J., et al. (2021). Whole-brain activation signatures of weight-lowering drugs. Mol. Metab. *47*, 101171. https://doi.org/10.1016/j.molmet.2021.101171.

12. Zhang, Q., Tenagne Delessa, C., Augustin, R., Bakhti, M., Colldén, G., Drucker, D.J., Feuchtinger, A., Garcia Caceres, C., Grandl, G., Harger, A., et al. (2021). The glucose-dependent insulinotropic polypeptide (GIP) regulates body weight and food intake via CNS-GIPR signaling. Cell Metab. *33*, 833–844.e5. https://doi.org/10.1016/j.cmet.2021.01.015.

13. Rudovich, N., Kaiser, S., Engeli, S., Osterhoff, M., Gögebakan, O., Bluher, M., and Pfeiffer, A.F.H. (2007). GIP receptor mRNA expression in different fat tissue depots in postmenopausal non-diabetic women. Regul. Pept. *142*, 138–145. https://doi.org/10.1016/j.regpep.2007.02.006.

14. Samms, R.J., Coghlan, M.P., and Sloop, K.W. (2020). How may GIP enhance the therapeutic efficacy of GLP-1? Trends Endocrinol. Metab. *31*, 410–421. https://doi.org/10.1016/j.tem.2020.02.006.

15. Campbell, J.E., Beaudry, J.L., Svendsen, B., Baggio, L.L., Gordon, A.N., Ussher, J.R., Wong, C.K., Gribble, F.M., D'Alessio, D.A., Reimann, F., et al. (2022). GIPR is predominantly localized to nonadipocyte cell types within white adipose tissue. Diabetes *71*, 1115–1127. https://doi.org/10.2337/db21-1166.

16. Hammoud, R., and Drucker, D.J. (2023). Beyond the pancreas: contrasting cardiometabolic actions of GIP and GLP1. Nat. Rev. Endocrinol. *19*, 201–216. https://doi.org/10.1038/s41574-022-00783-3.

17. McIntosh, C.H., Bremsak, I., Lynn, F.C., Gill, R., Hinke, S.A., Gelling, R., Nian, C., McKnight, G., Jaspers, S., and Pederson, R.A. (1999). Glucose-dependent insulinotropic polypeptide stimulation of lipolysis in differentiated 3T3-L1 cells: wortmannin-sensitive inhibition by insulin. Endocrinology *140*, 398–404. https://doi.org/10.1210/endo.140.1.6464.

18. Getty-Kaushik, L., Song, D.H., Boylan, M.O., Corkey, B.E., and Wolfe, M.M. (2006). Glucose-dependent insulinotropic polypeptide modulates adipocyte lipolysis and reesterification. Obesity (Silver Spring) *14*, 1124–1131. https://doi.org/10.1038/oby.2006.129.

19. Timper, K., Grisouard, J., Sauter, N.S., Herzog-Radimerski, T., Dembinski, K., Peterli, R., Frey, D.M., Zulewski, H., Keller, U., Müller, B., et al. (2013). Glucose-dependent insulinotropic polypeptide induces cytokine expression, lipolysis, and insulin resistance in human adipocytes. Am. J. Physiol. Endocrinol. Metab. *304*, E1–E13. https://doi.org/10.1152/ajpendo.00100.2012.

20. Weaver, R.E., Donnelly, D., Wabitsch, M., Grant, P.J., and Balmforth, A.J. (2008). Functional expression of glucose-dependent insulinotropic polypeptide receptors is coupled to differentiation in a human adipocyte model. Int. J. Obes. (Lond) *32*, 1705–1711. https://doi.org/10.1038/ijo.2008.148.

21. Lynggaard, M.B., Gasbjerg, L.S., Christensen, M.B., and Knop, F.K. (2020). GIP(3-30)NH2 - a tool for the study of GIP physiology. Curr. Opin. Pharmacol. *55*, 31–40. https://doi.org/10.1016/j.coph.2020.08.011.

22. Deacon, C.F., Nauck, M.A., Meier, J., Hücking, K., and Holst, J.J. (2000). Degradation of endogenous and exogenous gastric inhibitory polypeptide in healthy and in type 2 diabetic subjects as revealed using a new assay for the intact peptide. J. Clin. Endocrinol. Metab. *85*, 3575–3581. https://doi.org/10.1210/jcem.85.10.6855.

23. Coskun, T., Sloop, K.W., Loghin, C., Alsina-Fernandez, J., Urva, S., Bokvist, K.B., Cui, X., Briere, D.A., Cabrera, O., Roell, W.C., et al. (2018). LY3298176, a novel dual GIP and GLP-1 receptor agonist for the treatment of type 2 diabetes mellitus: from discovery to clinical proof of concept. Mol. Metab. *18*, 3–14. https://doi.org/10.1016/j.molmet.2018.09.009.

24. Samms, R.J., Christe, M.E., Collins, K.A., Pirro, V., Droz, B.A., Holland, A.K., Friedrich, J.L., Wojnicki, S., Konkol, D.L., Cosgrove, R.J., et al. (2021). GIPR agonism mediates weight-independent insulin sensitization by tirzepatide in obese mice. J. Clin. Invest. *131*, e146353. https://doi.org/10.1172/JCI146353.

25. Urva, S., Coskun, T., Loghin, C., Cui, X., Beebe, E., O'Farrell, L.S., Briere, D.A., Benson, C., Nauck, M.A., and Haupt, A. (2020). The novel dual glucose-dependent insulinotropic polypeptide and glucagon-like peptide-1 (GLP-1) receptor agonist tirzepatide transiently delays gastric emptying similarly to selective long-acting GLP-1 receptor agonists. Diabetes Obes. Metab. *22*, 1886–1891. https://doi.org/10.1111/dom.14110.

26. Borner, T., Geisler, C.E., Fortin, S.M., Cosgrove, R., Alsina-Fernandez, J., Dogra, M., Doebley, S., Sanchez-Navarro, M.J., Leon, R.M., Gaisinsky, J., et al. (2021). GIP receptor agonism attenuates GLP-1 receptor agonist-induced nausea and emesis in preclinical models. Diabetes *70*, 2545–2553. https://doi.org/10.2337/db21-0459.

27. Heise, T., DeVries, J.H., Urva, S., Li, J., Pratt, E.J., Thomas, M.K., Mather, K.J., Karanikas, C.A., Dunn, J., Haupt, A., et al. (2023). Tirzepatide reduces appetite, energy intake, and fat mass in people with type 2 diabetes. Diabetes Care *46*, 998–1004. https://doi.org/10.2337/dc22-1710.

28. Drucker, D.J. (2018). Mechanisms of action and therapeutic application of glucagon-like peptide-1. Cell Metab. *27*, 740–756. https://doi.org/10.1016/j.cmet.2018.03.001.

29. Kuzio, M., Dryburgh, J.R., Malloy, K.M., and Brown, J.C. (1974). Radioimmunoassay for gastric inhibitory polypeptide. Gastroenterology *66*, 357–364. https://doi.org/10.1016/S0016-5085(74)80134-4.

30. Nauck, M.A., El-Ouaghlidi, A., Gabrys, B., Hücking, K., Holst, J.J., Deacon, C.F., Gallwitz, B., Schmidt, W.E., and Meier, J.J. (2004). Secretion of incretin hormones (GIP and GLP-1) and incretin effect after oral glucose in first-degree relatives of patients with type 2 diabetes. Regul. Pept. *122*, 209–217. https://doi.org/10.1016/j.regpep.2004.06.020.

31. Song, D.H., Getty-Kaushik, L., Tseng, E., Simon, J., Corkey, B.E., and Wolfe, M.M. (2007). Glucose-dependent insulinotropic polypeptide enhances adipocyte development and glucose uptake in part through Akt activation. Gastroenterology *133*, 1796–1805. https://doi.org/10.1053/j.gastro.2007.09.005.

32. Mohammad, S., Ramos, L.S., Buck, J., Levin, L.R., Rubino, F., and McGraw, T.E. (2011). Gastric inhibitory peptide controls adipose insulin sensitivity via activation of cAMP-response element-binding protein and p110β isoform of phosphatidylinositol 3-kinase. J. Biol. Chem. *286*, 43062–43070. https://doi.org/10.1074/jbc.M111.289009.

33. Asmar, M., Simonsen, L., Madsbad, S., Stallknecht, B., Holst, J.J., and Bülow, J. (2010). Glucose-dependent insulinotropic polypeptide may enhance fatty acid re-esterification in subcutaneous abdominal adipose tissue in lean humans. Diabetes *59*, 2160–2163. https://doi.org/10.2337/db10-0098.

34. Eissing, L., Scherer, T., Tödter, K., Knippschild, U., Greve, J.W., Buurman, W.A., Pinnschmidt, H.O., Rensen, S.S., Wolf, A.M., Bartelt, A., et al. (2013). De novo lipogenesis in human fat and liver is linked to ChREBP-β and metabolic health. Nat. Commun. *4*, 1528. https://doi.org/10.1038/ncomms2537.

35. Allister, C.A., Liu, L.F., Lamendola, C.A., Craig, C.M., Cushman, S.W., Hellerstein, M.K., and McLaughlin, T.L. (2015). In vivo 2H2O administration reveals impaired triglyceride storage in adipose tissue of insulin-resistant humans. J. Lipid Res. *56*, 435–439. https://doi.org/10.1194/jlr.M052860.

36. Rotondo, F., Ho-Palma, A.C., Remesar, X., Fernández-López, J.A., Romero, M.D.M., and Alemany, M. (2017). Glycerol is synthesized and secreted by adipocytes to dispose of excess glucose, via glycerogenesis and increased acyl-glycerol turnover. Sci. Rep. *7*, 8983. https://doi.org/10.1038/s41598-017-09450-4.

37. Nye, C.K., Hanson, R.W., and Kalhan, S.C. (2008). Glyceroneogenesis is the dominant pathway for triglyceride glycerol synthesis in vivo in the rat. J. Biol. Chem. *283*, 27565–27574. https://doi.org/10.1074/jbc.M804393200.

38. Thomas, M.K., Nikooienejad, A., Bray, R., Cui, X., Wilson, J., Duffin, K., Milicevic, Z., Haupt, A., and Robins, D.A. (2021). Dual GIP and GLP-1 receptor agonist tirzepatide improves beta-cell function and insulin sensitivity in type 2 diabetes. J. Clin. Endocrinol. Metab. *106*, 388–396. https://doi.org/10.1210/clinem/dgaa863.

39. Rasouli, N., Molavi, B., Elbein, S.C., and Kern, P.A. (2007). Ectopic fat accumulation and metabolic syndrome. Diabetes Obes. Metab. *9*, 1–10. https://doi.org/10.1111/j.1463-1326.2006.00590.x.

40. Tan, C.Y., and Vidal-Puig, A. (2008). Adipose tissue expandability: the metabolic problems of obesity may arise from the inability to become more obese. Biochem. Soc. Trans. *36*, 935–940. https://doi.org/10.1042/BST0360935.

41. Merkel, M., Eckel, R.H., and Goldberg, I.J. (2002). Lipoprotein lipase: genetics, lipid uptake, and regulation. J. Lipid Res. *43*, 1997–2006. https://doi.org/10.1194/jlr.r200015-jlr200.

42. Hegele, R.A. (2016). Multidimensional regulation of lipoprotein lipase: impact on biochemical and cardiovascular phenotypes. J. Lipid Res. *57*, 1601–1607. https://doi.org/10.1194/jlr.C070946.

43. Ruscica, M., Ferri, N., Santos, R.D., Sirtori, C.R., and Corsini, A. (2021). Lipid lowering drugs: present status and future developments. Curr. Atheroscler. Rep. *23*, 17. https://doi.org/10.1007/s11883-021-00918-3.

44. Kim, S.-J., Nian, C., and McIntosh, C.H.S. (2007). Activation of lipoprotein lipase by glucose-dependent insulinotropic polypeptide in adipocytes. A role for a protein kinase B, LKB1, and AMP-activated protein kinase cascade. J. Biol. Chem. *282*, 8557–8567. https://doi.org/10.1074/jbc.M609088200.

45. Kim, S.-J., Nian, C., and McIntosh, C.H.S. (2010). GIP increases human adipocyte LPL expression through CREB and TORC2-mediated transactivation of the LPL gene. J. Lipid Res. *51*, 3145–3157. https://doi.org/10.1194/jlr.M006841.

46. Thondam, S.K., Daousi, C., Wilding, J.P.H., Holst, J.J., Ameen, G.I., Yang, C., Whitmore, C., Mora, S., and Cuthbertson, D.J. (2017). Glucose-dependent insulinotropic polypeptide promotes lipid deposition in subcutaneous adipocytes in obese type 2 diabetes patients: a maladaptive response. Am. J. Physiol. Endocrinol. Metab. *312*, E224–E233. https://doi.org/10.1152/ajpendo.00347.2016.

47. Bolsoni-Lopes, A., and Alonso-Vale, M.I.C. (2015). Lipolysis and lipases in white adipose tissue—an update. Arch. Endocrinol. Metab. *59*, 335–342. https://doi.org/10.1590/2359-3997000000067.

48. Christensen, M., Calanna, S., Sparre-Ulrich, A.H., Kristensen, P.L., Rosenkilde, M.M., Faber, J., Purrello, F., van Hall, G., Holst, J.J., Vilsbøll, T., et al. (2015). Glucose-dependent insulinotropic polypeptide augments glucagon responses to hypoglycemia in type 1 diabetes. Diabetes *64*, 72–78. https://doi.org/10.2337/db14-0440.

49. Heimburger, S.M.N., Nielsen, C.N., Calanna, S., Holst, J.J., Vilsbøll, T., Knop, F.K., and Christensen, M.B. (2022). Glucose-dependent insulinotropic polypeptide induces lipolysis during stable basal insulin substitution and hyperglycaemia in men with type 1 diabetes: A randomized, double-blind, placebo-controlled, crossover clinical trial. Diabetes Obes. Metab. *24*, 142–147. https://doi.org/10.1111/dom.14545.

50. Frayn, K.N. (1998). Non-esterified fatty acid metabolism and postprandial lipaemia. Atherosclerosis *141* (*Suppl 1*), S41–S46. https://doi.org/10.1016/s0021-9150(98)00216-0.

51. Finan, B., Ma, T., Ottaway, N., Müller, T.D., Habegger, K.M., Heppner, K.M., Kirchner, H., Holland, J., Hembree, J., Raver, C., et al. (2013). Unimolecular dual incretins maximize metabolic benefits in rodents, monkeys, and humans. Sci. Transl. Med. *5*, 209ra151. https://doi.org/10.1126/scitranslmed.3007218.

52. Joo, E., Harada, N., Yamane, S., Fukushima, T., Taura, D., Iwasaki, K., Sankoda, A., Shibue, K., Harada, T., Suzuki, K., et al. (2017). Inhibition of gastric inhibitory polypeptide receptor signaling in adipose tissue reduces insulin resistance and hepatic steatosis in high-fat diet-fed mice. Diabetes *66*, 868–879. https://doi.org/10.2337/db16-0758.

53. Mantelmacher, F.D., Zvibel, I., Cohen, K., Epshtein, A., Pasmanik-Chor, M., Vogl, T., Kuperman, Y., Weiss, S., Drucker, D.J., Varol, C., et al. (2019). GIP regulates inflammation and body weight by restraining myeloid-cell-derived S100A8/A9. Nat. Metab. *1*, 58–69. https://doi.org/10.1038/s42255-018-0001-z.

54. Clinicaltrials.Gov (2000). A study of LY3532226 in healthy participants. Identifier NCT04923269 (National Library of Medicine). https://clinicaltrials.gov/ct2/show/NCT04923269.

55. Clinicaltrials.Gov (2000). A research study looking at how well a combination of the medicines semaglutide and NNC0480-0389 works in people with type 2 diabetes. Identifier NCT05144984. https://clinicaltrials.gov/ct2/show/NCT05144984.

56. Clinicaltrials.Gov (2000). A study of LY3537021 in healthy participants and participants with type 2 diabetes mellitus. Identifier NCT04586907 (National Library of Medicine). https://clinicaltrials.gov/ct2/show/NCT04586907.

57. Knop, F.K., Urva, S., Rettiganti, M., Benson, C., Roell, W., Mather, K.J., Haupt, A., and Pratt, E.J. (2023). 56-OR: a long-acting glucose-dependent insulinotropic polypeptide receptor agonist shows weight loss without nausea or vomiting. Diabetes *72* (*Suppl 1*), 56-OR. https://doi.org/10.2337/db23-56-OR.

58. Carswell, K.A., Lee, M.J., and Fried, S.K. (2012). Culture of isolated human adipocytes and isolated adipose tissue. Methods Mol. Biol. *806*, 203–214. https://doi.org/10.1007/978-1-61779-367-7_14.

59. Basu, D., Manjur, J., and Jin, W. (2011). Determination of lipoprotein lipase activity using a novel fluorescent lipase assay. J. Lipid Res. *52*, 826–832. https://doi.org/10.1194/jlr.D010744.

60. Affymetrix. Microarray normalization using signal space transformation with probe guanine cytosine count correction. A White Paper from the Affymetrix. http://tools.thermofisher.com/content/sfs/brochures/sst_gccn_whitepaper.pdf.

61. Bolstad, B.M., Irizarry, R.A., Astrand, M., and Speed, T.P. (2003). A comparison of normalization methods for high density oligonucleotide array

data based on bias and variance. Bioinformatics *19*, 185–193. https://doi.org/10.1093/bioinformatics/19.2.185.

62. R Core Team (2018). R: A Language and Environment for Statistical Computing (R Foundation for Statistical Computing). https://www.R-project.org/.

63. Rensen, P.C., Herijgers, N., Netscher, M.H., Meskers, S.C., van Eck, M., and van Berkel, T.J. (1997). Particle size determines the specificity of apolipoprotein E-containing triglyceride-rich emulsions for the LDL receptor versus hepatic remnant receptor in vivo. J. Lipid Res. *38*, 1070–1084. https://doi.org/10.1016/S0022-2275(20)37190-X.

STAR★METHODS

KEY RESOURCES TABLE

REAGENT or RESOURCE	SOURCE	IDENTIFIER
Antibodies		
Anti-beta Actin	Cell Signaling Tech	4970S; RRID;AB_2223172
Anti-GIPR	Novus	NBP2-30085
Anti-phospho-ACC1	Cell Signaling Tech	3661S; RRID:AB_330337
Anti-phospho-HSL	Thermo Fisher	PA5-64494; RRID:AB_2662577
Goat anti-mouse IRDye 680	Licor	926-68070; RRID:AB_10956588
Goat anti-rabbit IRDye 800	Licor	925-32211; RRID:AB_2651127
Chemicals, peptides, and recombinant proteins		
DMEM	Gibco	Cat# 1054-020
^{13}C-acetate	Cambridge Isotope Lab	CLM-440-1
^{13}C-glucose	Cambridge Isotope Lab	CLM-1396-1
^{14}C-Glucose	Perkin Elmer	NEC042A
Adipocyte differentiation media	Zen Bio	DM2
Adipocyte maintenance media	Zen Bio	AM1
BODIPY 493/503 dye	Thermo Fisher	D3922
BSA	Gibco	11875
Butanol	Sigma	B7906
Chloroform	Acros	423555000
Collagenase Type I	Worthington	LS004197
Corn Oil	Sigma	Sigma C8267
Cytoclasin B	Sigma	C2743-200 uL
EGM-2MV Media	Lonza	CC-3202
EnzCheck substrate	Thermo Fisher	E33955
Ethanol	Decon Labs 2701	Decon Labs 2701, 200proof
fatty acid-free BSA	Thermo Fisher	3117057001
GIP	Eli Lilly and Co	2838382
GlutaMAX	Gibco	Cat# 35050
HEPES	Gibco	Cat# 15630
HGO buffer (Krebs-like buffer made at Eli Lilly and Co)	Eli Lilly and Co	BE06188-76
High-Capacity cDNA Reverse Transcription Kit	Thermo Fisher	4368814
Hoechst 33342 Nuclear Dye	Life Technologies	H3570
Insulin	Sigma	I9278-5ML
Isolectin IB4 Alexa Fluor 488	Thermo Fisher	I21411
Isopropanol	Sigma	19076-4
MES-SDS Buffer	Invitrogen	NP0002
Methanol	Thermo Fisher	A454-4
Microscint-E	Perkin Elmer	6013661
Odyssey Blocking Buffer	Licor	927-4000
PBS	Gibco	30256-01
Phosphatase Inhibitor Cocktail	Thermo Fisher	78428
Preadipocyte media	Zen Bio	PM1
Protease Inhibitor Cocktail	Thermo Fisher	1860932
RIPA Buffer	Pierce	89901
Sodium Hydroxide	Thermo Fisher	5425
Taqman 2X Universal PCR Master Mix	Thermo Fisher	4304437
Tirzepatide	Eli Lilly and Co	3298176

(*Continued on next page*)

Continued

REAGENT or RESOURCE	SOURCE	IDENTIFIER
Tris.HCl pH 8.0	Thermo Fisher	15568-025
Triton	Sigma	T8787
Tween-20	Sigma	P9416
Zwittergent	Sigma	41570
β-mercaptoethanol	Boston Bioproducts	BP-111R
Critical commercial assays		
BCA Protein Assay Kit	Pierce	23227
cAMP Dynamic 2 HTRF Assay Kit	CisBio	62AM4PEB
Fatty Acid Uptake Assay Kit	Molecular Devices	R8133
Lipolysis Assay Kit	Sigma	F6428
miRNeasy Mini Kit	Qiagen	1038703
SER473-AKT Assay Kit	CisBio	64AKSPEG
THR308-AKT Assay Kit	CisBio	64AKTPEG
Total AKT Assay Kit	CisBio	64NKTPEG
Triglyceride Assay kit	Roche Diagnostics	LS-K126
Experimental Organisms/strains		
Human subcutaneous preadipocytes	Zenbio	L020206
C57Bl/6 mice	Taconic or Janvier	9-10 weeks
DIO Mice	Taconic	C57/B16, 29-30 weeks
Software and algorithms		
Adobe Photoshop CC 2018	Adobe	N/A
GraphPad Prism	GraphPad Software	www.graphpad.com/scientific-software/prism/
Other		
384-well Taqman plates	Thermo Fisher	4309849
600 MHz Spectrometer NMR	Bruker	Avance III
96-Tissue Culture treated plates	Thermo Fisher	353219
ABI PRISM	Applied Biosystems	7900HT Sequence Detection System
Bis-Tris Gel	Novex	NP0322BOX
CytoStar-T plates	Perkin – Elmer	RPNQ0162
Isoplate	Perkin – Elmer	6005070
Microbeta counter	Perkin – Elmer	Model 2450
Modular Analyzer	Roche Diagnostics	Cobas 8000 modular analyzer with c502 chemistry module
Odyssey	Licor	CLx Infrared Imaging System
Synergy Neo2	BioTek	Neo2MAlphaB

RESOURCE AVAILABILITY

Lead contact

Further information and requests for resources and reagents should be directed to and will be fulfilled by the lead contact is Dr. William Roell, who can be reached at bill_roell@lilly.com.

Materials availability

Fluorescently labeled peptides generated in this study may be made available upon request but will require a completed Materials Transfer Agreement. Other reagents should be commercially available.

Data and code availability

Raw data generated in this study is available in the supplemental file, "Data S1 - Source Data". This paper does not report any original code. Any additional information required to reanalyze the data reported in this paper is available from the lead contact upon request.

EXPERIMENTAL MODEL AND STUDY PARTICIPANT DETAILS

- Human adipose tissue obtained from panniculectomy for whole adipose, stromal vascular fraction and adipocyte isolations as well as RNAscope and peptide incubation studies
- Mouse adipose obtained from diet induced obese C57BL/6 mice (Taconic 29-30 weeks old, weighing 47-55 g) used for whole adipose, stromal vascular fraction and adipocyte isolations as well as RNAscope and peptide incubation studies
- *In vivo* studies performed in C57BL/6 mice
- Human differentiated adipocyte model employed use of human preadipocytes from Zenbio and differentiated as detailed in methods

METHOD DETAILS

A list of all abbreviations used in this manuscript can be found in Table S1.

Adipocyte culture and differentiation

Primary adipose tissue was collected with tissue and adipocyte isolation and culture as previously described.[58] Differentiation of human adipocytes was performed using cryopreserved human subcutaneous preadipocytes from a single female donor (25 y, BMI 18.8) was obtained from Zenbio (L020206). Cells were expanded in EGM-2MV media (Lonza Cat#CC-3202). Preadipocytes were seeded (150,000/cm^2) on tissue culture treated surface in EGM-2MV media overnight and switched to preadipocyte media (Zen Bio Cat#PM-1). Cells were incubated overnight and replaced with differentiation media (Zen Bio Cat#DM-2). Media was replaced with fresh DM2 after third day followed by replacement with adipocyte media (Zen Bio Cat#AM-1) every third day for total culture time of 12-14 days. All experiments were conducted when the cells reached complete differentiation between 12-14 days.

Glucose Uptake

Preadipocytes were differentiated in CytoStar-T plates (Perkin Elmer Cat#RPNQ0162) for 12 days followed by overnight incubation in media without insulin (PM1 or DMEM/F12 (3:1) with 0.1% BSA). Media was replaced with 100 μL HGO buffer (see key resources table) + 1 mM glucose for 2 h. Cells were treated with 100 μL insulin (100 nM -100 fM) with and without 100, 10, 1 and 0.1 nM human native GIP or TZP (LY3298176) for 2 h. Media was replaced with 100 μL treatments in HGO buffer containing 100 μM glucose + 0.1 μCi ^{14}C-glucose (Perkin Elmer Cat#NEC042A) for 1 h followed by addition of cytoclasin B at 20 μM final concentration (Sigma Cat#C2743-200 μL). Radioactivity was counted in a microbeta counter (Perkin Elmer model #2450). Cytochalasin controls were subtracted as background counts.

Lipogenesis

Adipocytes were differentiated in Isoplate (PerkinElmer Cat#6005070) as described above. Cells were starved overnight in 100 μL Preadipocyte Media (Zenbio, Cat#PM-1). Cells were washed with 100 μL HGO buffer followed by treatment with insulin alone or insulin plus native human GIP or TZP as indicated above containing 10 μM glucose and 0.1 μCi ^{14}C-glucose (Perkin Elmer Cat#NEC042A) per well. After 4 h incubation, cells were washed twice with 150 μL PBS. Plates were inverted and gently tapped dry on an absorbent paper. Cells were lysed by gentle shaking for 5 min in 50 μL 0.5% Triton X-100 in water. 50 μL 2-butanol and 100 μL Microscint-E (Perkin Elmer Cat#6013661) was added followed by overnight incubation at room temperature to separate the aqueous/lipid phases with subsequent radioactivity counted (CPM) in the lipid phase to determine label incorporation into lipids.

Lipolysis

Differentiated adipocytes were incubated for 1 h in 100 μL DMEM (Dibco Cat#1054-020) containing 0.2% fatty acid free (FAF) BSA. Cells were washed and replaced with the same media (50 μL) containing treatments (insulin, GIP or TZP). 20 μL of conditioned media was removed after 3 h of incubation and free glycerol was measured using lipolysis reagent per vendor protocol (Sigma Cat#CF6428).

Protein Electrophoresis and Western Blot

Cells were lysed with cold RIPA buffer (Pierce Cat#89901) containing protease inhibitor (Thermo Cat#1860932) and phosphatase inhibitor (Thermo Cat#78428). Lysate was centrifuged at 6,000 g for 10 min to pellet the debris and total protein concentration of the supernatant was determined using BCA Protein Assay Kit (Pierce Cat#23227). Protein (10 μg) was denatured in Laemmli buffer containing 1.5% β-mercaptoethanol (Boston Bio Products Cat#BP-111R) for 10 min at 70°C. Samples were cooled on ice, quickly spun and loaded for electrophoresis in 1 mm 4-12% Bis-Tris gel (Novex Cat#NP0322BOX). Samples were run in MES-SDS Buffer (Invitrogen Cat # NP0002) at 200 V for 40 min. Gel was transferred onto PVDF membrane (Invitrogen, Cat#PVDF IB4010-02) for 8 min at 20 V using iblot transfer system (Invitrogen Cat#IB1001). Membrane was rinsed with deionized water twice for 1 min followed by blocking for 1 h in Odyssey Blocking Buffer (Licor Cat#927-4000). Membrane was incubated in 1:1000 dilution of anti-phospho-ACC1 (Cell Signaling, Cat#3661S), phospho-HSL (ThermoFisher Cat#PA5-64494), GIPR (Novus, Cat#NBP2-30085) or b-Actin (Cell Signaling, Cat#4970S) antibodies and 1:1 mix of PBS + 0.1% Tween-20 and Odyssey Blocking Buffer.

After overnight gentle shaking at 4°C, membrane was washed 3x 10 min in PBS + 0.1% Tween-20 followed by incubation at room temperature for 1 h in secondary antibody (Goat anti-rabbit IRDye 800 Licor Cat#925-32211 – 1:5000 or goat anti-mouse IRDye 680 Licor Cat#926-68070 – 1:5000) in 1:1 mix of PBS + 0.1% Tween-20 and Odyssey Blocking Buffer plus 0.01% SDS. Membranes were washed 3x 10 min in PBS + 0.1% Tween 20 and transferred to Odyssey Blocking Buffer. Membrane was scanned using Odyssey CLx Infrared Imaging System (Licor) at 700 and 800 setting.

RNA Isolation and cDNA synthesis

Flash frozen (500 mg) tissues were homogenized for 1-2 min in cold room in 1 mL Qiazol using Lysing Matrix D (MP Biomedicals Cat#116913500). Cultured adipocytes were homogenized using 100 μL Qiazol per 0.33 cm^2. Total mRNA was prepared using miRNeasy Mini Kit (Qiagen Cat#1038703). cDNA was synthesized from 500 ng total RNA in a 20 μL reaction using High Capacity cDNA Reverse Transcription Kit (Applied Biosystems Cat#4368814).

RT PCR

Relative mRNA was quantified using Taqman primer probes (See Taqman Probes Used, Applied Biosystems). cDNA was diluted 1:5 and RT-PCR was accomplished with Taqman 2X Universal PCR Master Mix (Applied Biosytems, Cat#4304437) in ABI Prism 7900HT Sequence Detection System (Applied Biosystems). Cycles for genes of interest was normalized to the housekeeping gene PPIA. Taqman probes utilized are listed in Table below.

Taqman Probes Used

(All Taqman probes obtained from Applied Biosystems)

Gene	Taqman Probe Id	Gene	Taqman Probe Id	Gene	Taqman Probe Id
ACO2	Hs00426616_g1	FABP4	Hs01086177_m1	NDUFA8	Hs00204417_m1
ACC1	Hs01046047_m1	FASN	Hs01005622_m1	NDUFAB1	Hs00192290_m1
ADIPOQ	Hs00605917_m1	FOXO1	Hs00231106_m1	NDUFB6	Hs05526838_s1
AGPAT1	Hs00965850_g1	GIPR	Hs00609210_m1	NDUFS2	Hs00190020_m1
AGPAT2	Hs00944961_m1	GLPR	Hs00157705_m1	NDUFS8	Hs00159597_m1
ATGL	Hs00982040_g1	GLUT4	Hs00168966_m1	NDUFV1	Hs00957930_m1
ATP5A1	Hs00900735_m1	GPAT2	Hs04961945_g1	OGDH	Hs01081865_m1
ATP5B	Hs00969569_m1	HSL	Hs00193510_m1	PGC1a	Hs00173304_m1
ATP5D	Hs00961521_m1	IDH1	Hs04966974_g1	PPARa	Hs00947536_m1
ATP5G1	Hs00829069_s1	IDH2	Hs00953879_m1	PPARg	Hs00234592_m1
ATP5G3	Hs00909659_m1	IDH3A	Hs00194253_m1	PPIA	Hs04194521_s1
CEBPa	Hs00269972_s1	IDH3G	Hs01021749_g1	SDHB	Hs01042481_m1
CEBPb	Hs00270923_s1	INSR	Hs00961561_m1	SDHD	Hs00829723_g1
CEBPd	Hs00270931_s1	LIPIN1	Hs00299515_m1	SREBP1	Hs01088691_m1
COX5A	Hs00362067_m1	LPL	Hs00173425_m1	SREBP2	Hs01081784_m1
COX5B	Hs00426950_g1	MDH2	Hs00938918_m1	SUCLA2	Hs01597886_g1
COX7B	Hs00371307_m1	MGL	Hs00996004_m1	UQCRC1	Hs00163415_m1
COXA8	Hs00187909_m1	MTND2	Hs02596874_g1	UQCRFS1	Hs04194251_g1
CREB	Hs00231713_m1	NDUFA12	Hs00984333_m1	UQCRH	Hs03045181_g1
DLD	Hs00355675_m1	NDUFA5	Hs01634019_g1		
DLST	Hs04276516_g1	NDUFA6	Hs00899690_m1		

cAMP Assay

Differentiated adipocytes were washed with 100 μL HGO + 2 mM glucose + 500 μM IBMX. Cells were treated with Insulin, native human GIP or TZP (100 nM - 1 fM) for 30 min in the same media. cAMP was determined using cAMP HTRF Kit (Cisbio Cat#62AM4PEB).

Total and phospho-AKT Assay

Differentiated adipocytes were incubated overnight in 100 μL PM1, followed by incubation in 100 μL phenol red-free DMEM-F12(3:1) + 0.1% BSA for 2 h. Cells were treated 100 nM-5 fM native human GIP, TZP or Insulin in 100 μL HGO buffer without any proteins for 3-5 min. Cells were processed of phosphorylated AKT (SER473-AKT, Cisbio Cat#64AKSPEG and THR308-AKT, Cisbio Cat#64AKTPEG) or Total AKT (Cat#64NKTPEG) per vendor protocol. HTRF ratios were normalized to time matched total AKT.

Fatty Acid uptake Assay

Differentiated adipocytes were incubated overnight in 100 μL PM1. Cells washed once with 100 μL HGO buffer and incubated at 37°C for 1 h in 50 μL of HGO buffer followed by treatment with 50 μL of 2X Insulin, GIP or TZP (1 fM-100 nM) for 30 min. 100 μL of fatty acid reagent in HGO buffer added per vendor protocol (Molecular Devices, QBT Fatty Acid Uptake Assay Kit, Cat#R8133). Fluorescence (485EX/515EM) was recorded using Synergy Neo2 (BioTek) after 15 min to measure fatty acids that were taken up by the adipocytes.

LPL Assay

Differentiated adipocytes were incubated overnight in 100 μL PM1. Media was replaced with 100 μL DMEM + 5.5 mM glucose + 0.1% fatty acid-free (FAF)-BSA for 2 hr followed by replacement with similar media containing treatments (100 μL Insulin, GIP or TZP) for for 5 hr. 20 μL conditioned media was assayed for LPL activity as described by Basu et al.[59]

^{13}C-Glycerol measurement by NMR

Adipocytes were differentiated in 6-well tissue culture treated dishes and media was replaced with PM1 overnight. Cells were treated with 100 nM Insulin, GIP or TZP for 24 h with 500 μM ^{13}C-acetate plus 5.5 mM glucose or with 5.5 mM ^{13}C-glucose in DMEM plus 2.5% FAF-BSA. Cells were washed 3X with PBS and pellet was resuspended in 9:1 IPA:$CHCl_3$. After vigorous mixing, half the sample was subjected to overnight saponification (0.1 M NaOH/methanol, 1:1 v/v). Dried residue was resuspended in 800 μL deuterium oxide (Sigma Cat#151882) and neutralized with 200 μL of 5% acetic acid. Unsaponified samples were processed similarly except NaOH was absent. After brief centrifugation to sediment the debris, solution was analyzed for total ^{13}C-glycerol.

Exome Array Analysis

Adipocytes were differentiated as previously described and subsequently treated with insulin (100 nM), GIP (100 nM), insulin + GIP, or vehicle for 2, 8, and 24 h. RNA was collected and submitted for transcriptomic analysis utilizing the ThermoFisher Human Clariom S Assay platform. The CEL files of 36 samples were processed via GC-SST-RMA[60] and then followed by the quantile normalization method[61] to get the normalized mRNA expression data. Principal component analysis (PCA) and outlier analysis were applied to check any potential pattern or outliers among the samples. The one-way ANOVA using R software.[62] R: A language and environment for statistical computing. R Foundation for Statistical Computing) was applied to the normalized mRNA expression to test the comparisons between each treatment and vehicle. For each comparison, both the p values and the fold changes were reported, and the mRNAs with p value less than 0.05 and fold change no less than 1.5 were selected for further analysis. Gene sets for metabolic pathways were hand-curated using the Ingenuity Pathway Analysis (IPA) tool, the Kyoto Encyclopedia of Genes (KEGG) database and literature information. Additional analytics were performed using the TIBCO Spotfire tool.

Trace fluorescently labeled molecules

Mouse and human adipose tissue were freshly isolated using previously described protocol.[58] AZDye647-labeled TZP (TZP-FL: 10-100 nM), AZDye647-labeled GIPRA (GIPRA-FL: 300-1000 nM), and AZDye647-labeled Exendin-4 (Ex4-FL: 100-1000 nM) were incubated for 60 min. Then, tissues were washed with PBS to remove unbound fluorescence then immediately fixed in 4% paraformaldehyde for 30 min. Subsequently tissue was incubated with 1 μM Bodipy 493, 5 μg/mL Isolectin GS-IB4-Alexa Fluor 568, and 1 μg/mL Hoechst 33342 for 30 minutes and washed with PBS. Adipose tissues were imaged z-stack using a Zeiss LSM800 confocal microscope with 20x objective (Carl Zeiss Microscopy). 3-dimensional images were rendered by Imaris 9.2.1 (Bitplane).

In Vivo Experiments

All experiments were performed in accordance with the Institute for Laboratory Animal Research Guide for the Care and Use of Laboratory Animals or had received approval from the Ethical Review Board for Animal Experimentation of the Leiden University Medical Center, Leiden, the Netherlands, and Eli Lilly and Company Institutional Animal Use and Care Committee.

Body Weight and Composition in Diet-induced Obese Mice

Food intake and weight in DIO male C57BL/6 mice (Taconic Biosciences, Rensselaer, NY) 29-30 weeks old, weighing 47-55 g were used. Animals were individually housed in a temperature-controlled (24°C) facility with a 12-hour light/dark cycle (lights on 10 PM), and had free access to food TD95217 (Teklad) and water. After 2 weeks acclimation to the facility, mice were randomized to treatment groups (n=5/group) based on body weight so each group has similar starting mean body weight. On days -2 and 15, total fat mass was measured by nuclear magnetic resonance (NMR) using an Echo Medical System (Houston, TX) instrument. Vehicle (40 mM Tris-HCl, pH 8.0), or a long-acting GIP analogue (GIPFA-085, 1000 nmol/kg) were subcutaneously administered to *ad libitum* fed DIO mice 30–90 min prior to the onset of the dark cycle as daily (QD) beginning on day 1. Daily body weight and food intake were measured throughout the study. At the end of the study blood was collected for glucose, insulin, and triglyceride analysis.

Acute Oral Lipid Challenge in Lean Mice

Male C57BL/6 mice sourced from (Taconic Biosciences, Rensselaer, NY) were utilized for the studies. The mice were singularly housed in HD rodent cages on a 12:12 normal light cycle 6 PM to 6 AM Dark. Mice were maintained on Teklad 2014 lab animal

diet (Envigo, Indianapolis, IN) prior to the start of the study. Animals received house water *ad libitum* throughout the study. Serum was prepared from all blood collections and triglycerides were measured using a Cobas 8000 modular analyzer with c502 chemistry module (Roche Diagnostics, Indianapolis, IN).

Prior to study start mice were weighed and blood was collected from the retro-orbital sinus under isoflurane anesthesia. Serum triglycerides were measured and animals were randomized into groups of similar serum triglycerides and body weights (n=9-12). Nine hours into the light cycle on day 0 animals were dosed SQ with LAGIPRA (GIPFA-085) or vehicle and fasted. Approximately one to two hours into the light cycle on Day 1 the mice were weighed and dosed by oral gavage at 10 mL per kg body weight with a corn oil to ethanol emulsion (9:1, v/v). Three hours into the light cycle (1 h after emulsion administration) mice were bled under isoflurane anesthesia from the retro-orbital sinus and dosed by oral gavage with 100% corn oil at 20 mL per kg body weight. Blood was collected from animals under isoflurane anesthesia via the retro-orbital sinus at 1 and 2 h after the 100% corn oil administration and a 4 h terminal sample was collected by cardiac puncture. In some studies, Tyloxapol (Sigma) was administered retro-orbitally at 300 mg/kg body weight under isoflurane anesthesia at the same time the 100% corn oil was administered. Stomachs were collected after the terminal blood collection and stomach content was weighed.

Triglycerides Assessment after Semi-Chronic Repeat Dose in Lean Mice

Prior to study start mice were weighed and blood was collected from the retro-orbital sinus under isoflurane anesthesia. Triglycerides were measured and animals were randomized into groups of similar triglycerides and weights (n=10). On day 1 at approximately 1 h into the light cycle mice were dosed with LAGIPRA or vehicle subcutaneously. On days 2, 3 and 4 blood was collected from the retro-orbital sinus approximately 1 h into the light cycle and LAGIPRA or vehicle were administered subcutaneously. On day 4, 6 h after the LAGIPRA or vehicle administration, mice were anesthetized with isoflurane anesthesia and a terminal blood collection was performed by cardiac puncture.

Organ uptake of triglyceride-rich lipoprotein-mimicking particles in Lean Mice

12-week-old male C57BL/6J mice (Janvier Labs, Le Genest-Saint-Isle, France) were housed in conventional cages with a 12:12 h light-dark cycle and *ad libitum* access to regular chow diet (Rat and Mouse No. 1 Maintenance; Special Diets Services, Witham, United Kingdom) and water.

Body weight was determined, based on which mice were divided into 3 groups of 10 mice. At 9:30 PM clock time, corresponding to Zeitgeber time (ZT) 14.5, mice received a single subcutaneous injection (approx. 100 μL) with either LAGIPRA (GIPFA-085; 300 nmol/kg body weight), a LAGLP-1RA (GLP-140; 30 nmol/kg body weight) or vehicle (0.02% Tween80 in 20 mM Tris.HCl).

The next day, mice were fasted for 6 h (7:00 AM to 1:00 PM clock time, corresponding to ZT 0 to 6). At 1:30 PM clock time, corresponding to ZT 6.5, mice were intravenously injected with 80 nm-sized glycerol tri[^{3}H]oleate-labeled triglyceride-rich lipoprotein (TRL)-like particles,[63] at a dose of 1.0 mg triglyceride in 200 μL PBS per mouse. After 15 min, mice were sacrificed by CO_2 inhalation and perfused with ice-cold PBS to remove blood from organs. Subsequently, gonadal white adipose tissue (gWAT) was isolated, weighed and part (approx. 50-150 mg) was dissolved overnight at 56°C in 0.5 mL Tissue Solubilizer (Amersham Biosciences, Roosendaal, the Netherlands). Dissolved tissues were mixed with 5 mL Ultima Gold scintillation fluid (PerkinElmer, Groningen, The Netherlands) and ^{3}H activity was determined in a liquid scintillation counter. Disintegrations per minute of ^{3}H were expressed as percentage of the injected dose per gram tissue and per whole organ.

Calorimetry in DIO mice

Diet-induced obese (DIO) male C57/Bl6 mice (Taconic Biosciences, Cambridge City, IN) 24 weeks to 25 weeks old, maintained on a calorie-rich diet since arrival at Lilly (TD95217), were used in the following studies. Animals were individually housed in a temperature-controlled (24°C to 27°C) facility with a 12-h light/dark cycle (lights on 22:00) and free access to food and water.

After a minimum of 2 weeks acclimation to the facility, the mice were placed in TSE PhenoMaster/LabMaster calorimeter for 3 days of acclimation and were performed at thermoneutrality (27°C). Mice were randomized according to their body weight, so each experimental group of animals would have similar body weight. Mice body weight ranged from 43 g to 50 g. All groups contained 6 mice. Vehicle (20 mM Tris-HCl at pH 8.0), Semaglutide (1nmol/kg), LAGIP (100nmol/kg) or combination (Semaglutide + LAGIP) dissolved in vehicle was administered by subcutaneous (SC) injection (10 mL/kg) to ad libitum-fed DIO mice 30 min–90 min prior to the onset of the dark cycle daily. Body weight and food intake were measured daily throughout the study. Absolute changes in body weight were calculated by subtracting the body weight of the same animal prior to the first injection of molecule. Heat and respiratory exchange ratio (RER) were measured by indirect calorimetry using an open-circuit calorimetry system. RER is the ratio of the volume of CO2 produced (VCO2) to the volume of O2 consumed (VO2). Heat was calculated with full body weight considered:

- VO2 = FlowML× (V1+V2)/N2Ref×Animal weight×100)
- VCO2 = FlowML×dCO2/Animal weight×100)
- Heat = (CVO2×VO2+CVCO2×VCO2)/1000;
- where CVO2 = 3.941; CVCO2 = 1.106

All data were presented as mean ± SEM of 6 animals per group. Statistical analysis was performed using repeated measures ANOVA, followed by Dunnett's or Tukey's method for multiple comparisons. Significant differences were identified at $p < 0.05$.

General animal health and welfare was monitored by veterinary staff in all studies. No adverse effects were reported.

Hyperinsulinemic/euglycemic clamp studies

A euglycemic clamp study in male, diabetic Sprague-Dawley rats was performed to understand the overall in vivo activity of native GIP and LAGIPRA on glucose utilization. Male Sprague-Dawley rats (Taconic Biosciences, Rensselaer, NY), 275 to 300 grams, were acclimated to the facility with 12:12 hour light (0600 on and 1800 off) and fed regular chow and house water ad libitum. Animals were anesthetized with isoflurane and sterile catheters were placed in the left carotid and right jugular vein. Streptozotocin (45mg/kg) was prepared just prior to use by dissolving in 100 mM sodium citrate buffer, pH 4.5 and was administered through the arterial catheter. All animals were monitored for general recovery and were placed on 5% glucose-house water for the first two days to prevent hyperinsulinemia-induced hypoglycemia. Seven to eight days post-surgery, the catheters were exteriorized, and animals were allowed to acclimate to the study boxes for a minimum of one hour.

A bolus/continuous infusion of 3-3H-glucose was initiated in overnight-fasted rats to determine endogenous glucose production (EGP) under basal conditions. An intravenous infusion of Vehicle, native hGIP-NH2 or LAGIPRA was then administered (n=8 per group).

- Native hGIP-NH2: 12pmol/kg/in
- LAGIPRA: 48pmol/kg/min

An insulin infusion (5mU/kg/min) was initiated and a variable intravenous infusion of 45% glucose was started and periodically adjusted to maintain blood glucose concentration at 110-120 mg/dL. Somatostatin was administered to inhibit endogenous insulin secretion. Arterial blood samples were obtained during the experiment to monitor hematocrit, plasma insulin, and C-peptide, and basal and clamp period endogenous glucose production (EGP). At the end of the experiment, 2-[1-14C]-deoxyglucose was administered to measure tissue glucose uptake in tissues snap frozen in liquid nitrogen under steady state glucose concentrations.